Table 2
IC_{50} of ADR-conjugated PEG-modified dendrimers for HeLa cells

Dendrimer	IC_{50} (μM)[a]	
	Amide	Hydrazone
PEG–Glu-G4	60.2 ± 3.8	8.7 ± 1.5
PEG–Glu-G0	12.4 ± 3.5	12.1 ± 2.0

[a] IC_{50} of free ADR was 1.6 ± 0.3.

and intercalate into DNA to express cytotoxic activity [14,15,31]. We next examined intracellular localization of adriamycin carried by these conjugates. HeLa cells were treated with the adriamycin-conjugated PEG-modified dendrimers for 1 h and were washed with PBS. The cells were incubated in a culture medium for 5 h and then observed using a fluorescence microscope.

As portrayed in Fig. 6A, the cells treated with free adriamycin displayed fluorescence in the nucleus. However, fluorescence of adriamycin for the cells treated with the PEG-modified dendrimer bearing adriamycin through amide bond differed greatly from the fluorescence of cells treated with free adriamycin (Fig. 6B, C). Fluorescence of adriamycin was visible in both the cytoplasmic space and the nucleus for cells treated with the PEG-G0 conjugate, although fluorescence was not visible for cells treated with PEG–Glu(ADR)-G4. This observation suggests that the entrance of adriamycin bound to PEG–Glu(ADR)-G4 was restricted by the PEG-modified dendrimer but that adriamycin bound to small G0 dendrimer can enter the nucleus.

In contrast, cells treated with the PEG-modified dendrimers bearing adriamycin via hydrazone bond displayed marked fluorescence in the nucleus (Fig. 6D, E). Considering that PEG-modified G4 dendrimer–adriamycin conjugate with amide bond did not enter the nucleus (Fig. 6C), this result indicates that the dendrimer–adriamycin conjugates with hydrazone linkage released the drug molecules inside cells. These conjugates might be trapped in endosomes and lysosomes after their internalization into the cell. The acidic environment of these subcellular compartments then triggered cleavage of hydrazone linkage and enabled the drug molecules to enter the nucleus [14,15].

3.5. Cytotoxicity of adriamycin-bearing PEG-modified dendrimers against adriamycin-sensitive and ADR-resistant cells

We next examined the cytotoxicity of adriamycin-sensitive and -resistant cancer cells: SBC-3 and SBC-3/ADM100. The latter cells were established by the selection of human lung SBC-3 cells in adriamycin-containing medium. These cells highly expressed MDR-1, which plays an important role in multidrug resistance (MDR) [29]. Fig. 7 depicts cell viability after incubation with the adriamycin-bearing PEG-modified dendrimers or free adriamycin. Free adriamycin was much less effective to adriamycin-resistant SBC-3/ADM100 cells than SBC-3 cells. However, these adriamycin-bearing PEG-modified dendrimers expressed the same level of toxicity toward both adriamycin-sensitive and adriamycin-resistant cells. Relative resistance was defined as the ratio of IC_{50} of free or dendrimer-conjugated adriamycin for the adriamycin-sensitive cell to that for adriamycin-resistant cell (Table 3). Relative resistance for free adriamycin was 58.7, whereas that for the dendrimer-conjugated adriamycin was 1–2.8. This result indicates that these adriamycin-bearing dendrimers act on adriamycin-resistant cells with almost equal efficacy to that of the adriamycin-sensitive cells. Among these adriamycin-bearing dendrimers, PEG–Glu(NHN–ADR)-G4 exhibited the highest cytotoxic activity against SBC-3/ADM100 cells, suggesting that the PEG-modified dendrimers that carry many adriamycin molecules and release them inside the cell can achieve an efficient therapeutic effect.

4. Discussion

For this study, we synthesized four kinds of adriamycin-conjugated PEG-modified dendrimers with different generations of dendrimers and with different linkage for adriamycin conjugation: PEG–Glu(ADR)-G0, PEG–Glu(ADR)-G4, PEG–Glu(NHN–ADR)-G0, and PEG–Glu(NHN–ADR)-G4. The dendrimers with adriamycin via amide bond were very stable and released no adriamycin under neutral and mildly acidic conditions. The PEG-modified dendrimers with adriamycin via hydrazone bond also retained adriamycin molecules at neutral pH, although adriamycin molecules were released from the dendrimers at pH 5.5, which corresponds to endosomal environment (Fig. 4).

As shown in Fig. 5, PEG–Glu(NHN–ADR)-G4 exhibited much higher cytotoxicity than PEG–Glu(ADR)-G4. Probably, PEG–Glu(NHN–ADR)-G4 is taken up by the cell through endocytosis and is subsequently trapped in a subcellular acidic compartment, such as endosome and lysosome. Then, the acidic environment might induce cleavage of hydrazone linkage; liberated adriamycin molecules enter the nuclei, which is consistent with previous observations [14,15]. Actually, HeLa cells treated with PEG–Glu(NHN–ADR)-G4 exhibited adriamycin fluorescence in nuclei, but the same cells treated with PEG–Glu(ADR)-G4 displayed only slight fluorescence in nuclei (Fig. 5). These results indicate that acid-labile hydrazone linkage is necessary for the large adriamycin-conjugated dendrimers to express high cytotoxic activity. In contrast, the small adriamycin-bearing PEG-modified dendrimers demonstrated a different situation: PEG–Glu(NHN–ADR)-G0 exhibited almost the same cytotoxicity as PEG–Glu(ADR)-G0. This result suggests that the small adriamycin–dendrimer conjugates can reach the site of action, irrespective of the cleavability of the drug–dendrimer linkage.

Because the endocytotic pathway is a major route by which cells take up large molecules and particles, it is likely that adriamycin-conjugated PEG-modified dendrimers were taken up by endocytosis and were subsequently trapped in the endosomal compartment, which has a weakly acidic environment. Poly(amidoamine) dendrimers are known to induce rupture of endosomes through a so-called proton sponge effect [32].

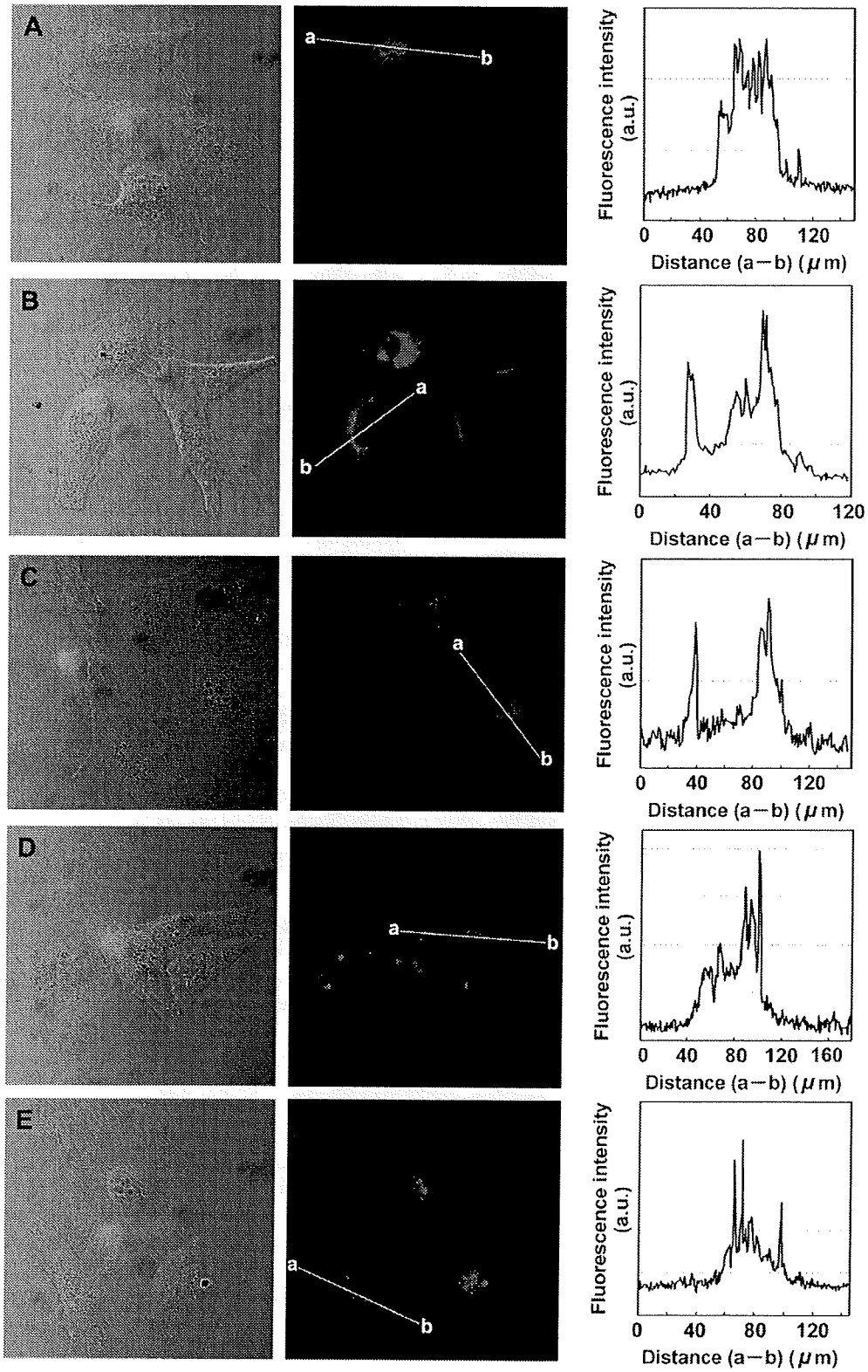

Fig. 6. Differential interference images (left) and fluorescence images (center) of HeLa cells treated with free adriamycin (A), PEG–Glu(ADR)-G0 (B), PEG–Glu(ADR)-G4 (C), PEG–Glu(NHN–ADR)-G0 (D) and PEG–Glu(NHN–ADR)-G4 (E). Fluorescence intensity profiles along the line a–b shown in the fluorescence images were also given (right panel).

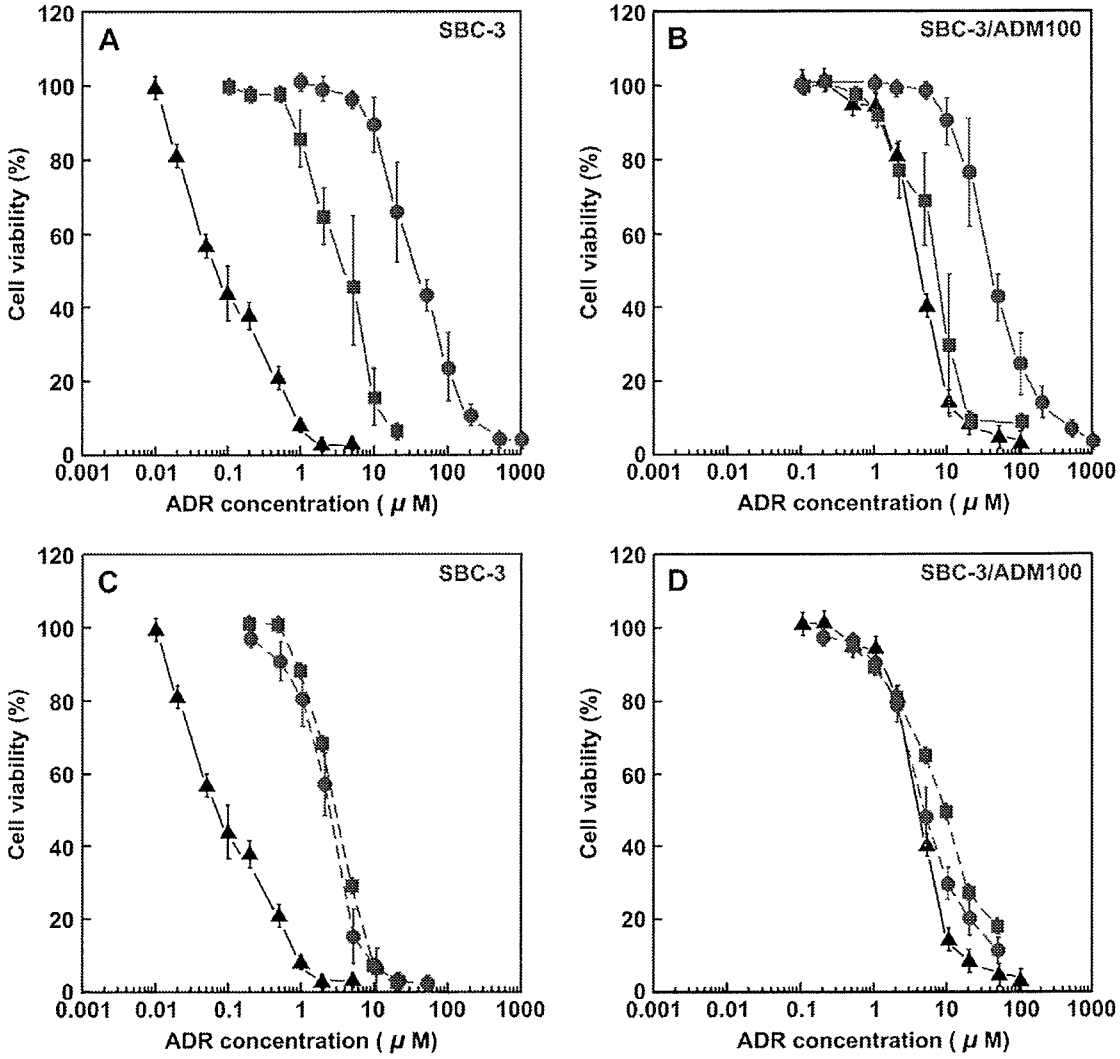

Fig. 7. Cytotoxicity of free adriamycin (triangles), PEG–Glu(ADR)-G0 (squares), and PEG – PEG–Glu(ADR)-G4 (circles) to SBC-3 (A) and SBC-3/ADM100 cells (B). Cytotoxicity of free adriamycin (triangles), Glu(NHN–ADR)-G0 (squares), and PEG–Glu(NHN–ADR)-G4 (circles) to SBC-3 (C) and SBC-3/ADM100 cells (D). Cell viability was expressed as the percentage of the untreated control cells.

For that reason, these adriamycin-conjugated PEG-modified dendrimers might transfer from endosome to cytosol.

Small molecules with less than 6 nm or 60 kDa, such as green fluorescent protein, are known to be able to permeate through nuclear pores, but larger molecules cannot [33]. Using dynamic light scattering, we estimated the PEG–Glu(OBzl)-G4 dendrimer diameter to be about 12 nm; consequently, the adriamycin-bearing PEG-G4 dendrimers were unable to enter the nucleus (Fig. 6). For that reason, liberation of adriamycin molecules from the dendrimer might be necessary for elicitation of their high cytotoxicity. However, the adriamycin-bearing PEG-modified G0 dendrimers might be sufficiently small to permeate nuclear pores and reach the genomic DNA. In fact, fluorescence of adriamycin was apparent for cells treated with these adriamycin-bearing PEG-modified G0 dendrimers, irrespective of the type of adriamycin–dendrimer linkage (Fig. 6B, D).

Considering that cancer chemotherapy is limited by the MDR of cancer cells, it is noteworthy that the adriamycin-conjugated PEG-modified dendrimers exhibited almost equivalent

Table 3
Cytotoxicity of ADR-conjugated PEG-modified dendrimers for SBC-3 and SBC-3/ADM cells

Conjugate	IC_{50} (μM)		Relative resistance[a]
	SBC-3	SBC-3/ADM100	
Free ADR	0.075 ± 0.015	4.4 ± 0.1	58.7
PEG–Glu(ADR)-G0	3.3 ± 1.9	7.5 ± 2.0	2.3
PEG–Glu(NHN–ADR)-G0	3.4 ± 0.1	9.6 ± 0.1	2.8
PEG–Glu(ADR)-G4	40.3 ± 10.9	41.2 ± 8.4	1.0
PEG–Glu(NHN–ADR)-G4	2.5 ± 0.5	4.9 ± 1.1	2.0

[a] Mean ratio of IC_{50} for SBC-3 to that for SBC-3/ADM100.

cytotoxic activity to adriamycin-resistant SBC-3/ADM100 cells as to adriamycin-sensitive SBC-3 cells (Fig. 7, Table 3). Also, MDR is acquired by the ability to pump drug molecules out of the cell [34]. Efflux transporters, such as P-glycoprotein and MDR-associated proteins, are known to be involved in MDR [35,36]. It is likely that adriamycin excretion depends on the route of cellular uptake and intracellular localization. Free adriamycin penetrates the plasma membrane through simple diffusion [14,15,31]. In contrast, adriamycin-conjugated PEG-modified dendrimers might be taken up by cells via endocytosis and moved to endosomal vesicles in cells. Such a difference of cellular internalization mechanisms might affect the accessibility of efflux transporters to adriamycin molecules, resulting in high toxicity of the dendrimer–adriamycin conjugates toward the adriamycin-resistant cells. In fact, superior cytotoxic activity of macromolecular drugs to low-molecular-weight drugs against MDR cells has already been observed for various polymer–drug conjugates [36–39]. These polymeric drugs are taken up by the cell through endocytosis and avoid pumping out by efflux transporters.

Minko et al. prepared a polymer–drug conjugate in which adriamycin residues were connected to *N*-(2-hydroxypropyl)-methacrylamide (HPMA) copolymer through a lysosomally degradable oligopeptide linkage. They compared its cytotoxicity with adriamycin-sensitive A2780 cells and adriamycin-resistant A2780/AD cells (human ovarian carcinoma cell lines) and reported that the conjugate exhibited similar cytotoxicities to these cells with IC_{50} around 40 μM, in contrast to free ADR, which showed a 38-times higher IC_{50} value toward A2780/AD cells ($IC_{50} = 6.92$ μM) than toward A2780 ($IC_{50} = 0.18$ μM) [36]. Direct comparison of cytotoxic potency between the HPMA copolymer–adriamycin conjugate and our adriamycin-conjugated PEG-modified dendrimers is difficult because of the difference of the cells used for estimation of cytotoxicity. However, the comparison based on IC_{50} implies that our conjugates may possess equivalent or higher cytotoxic potency against MDR cells, despite differences in the linkages of drug conjugation and molecular architectures between these polymer–drug conjugates.

Polymer–drug conjugates are widely used as components of polymeric micelles that accumulate at tumor tissues through the EPR effect [40–42]. Bae et al. conjugated a block copolymer of PEG and poly(aspartate) with adriamycin via hydrazone linkage and prepared polymeric micelles from this polymer–adriamycin conjugate with amphiphilic nature. They showed that after internalization into a cell through endocytosis, the polymeric micelles released adriamycin in endosome, and exhibited cytotoxic activity in a time-dependent manner [43]. Indeed, this polymeric micelle, along with various polymeric micelles of other types, has been shown to exhibit antitumor activity *in vivo* [44]. Polymeric micelles are formed by self-assembly of amphiphilic polymers in the medium and are necessarily larger, with broader distribution than dendrimer-based carriers. How such different sizes and distributions affect extravasation, renal excretion, translocation in the interstitial space, possible nuclear entry, and therapeutic efficacy remain to be clarified.

5. Conclusion

We synthesized and characterized four adriamycin-conjugated PEG-modified PAMAM dendrimers: PEG–Glu(ADR)-G0, PEG–Glu(ADR)-G4, PEG–Glu(NHN–ADR)-G0, and PEG–Glu(NHN–ADR)-G4. The adriamycin-conjugated dendrimers with hydrazone bonds were stable under physiological conditions, and adriamycin molecules were released from PEG-modified dendrimers in acidic environments such as those of endosomes/lysosomes. We demonstrated that these conjugates with hydrazone bonds exhibited higher cytotoxic effects than those with amide bonds. Results of this study showed that these adriamycin-conjugated PEG-modified dendrimers were effective even for MDR cancer cells. It is noteworthy that the PEG-modified G4 dendrimer having adriamycin residues through hydrazone linkage exhibited comparable cytotoxicity to that of free adriamycin toward both adriamycin-sensitive and adriamycin-resistant cells. Indeed, further optimization of the structure of the dendrimer–ADR conjugates is necessary to improve their cytotoxic activity. However, this type of dendrimer–ADR conjugates with the uniform size and the highly hydrated surface could exhibit much more efficient accumulation through an EPR effect, compared to free ADR. Information obtained in this study is expected to be useful for development of dendrimer-based carriers for accurate drug delivery.

Acknowledgements

This work was supported in part by Grant-in-Aid for Research on Nano-technical Medicine from the Ministry of Health, Labor and Welfare of Japan and Grants-in-aid from the Ministry of Education, Science, Sports and Culture of Japan.

References

[1] Vicent M, Duncan R. Polymer conjugates: nanosized medicines for targeting cancer. Trends Biotechnol 2006;24:39–47.
[2] Duncan R. Polymer conjugates as anticancer nanomedicines. Nat Rev Cancer 2006;6:688–701.
[3] Haag R, Kratz F. Polymer therapeutics: concepts and applications. Angew Chem Int Ed 2006;45:1198–215.
[4] Maeda H, Wu J, Sawa T, Matsumura Y, Hori K. Tumor vascular permeability and the EPR effect in macromolecular therapeutics: a review. J Control Release 2000;65:271–84.
[5] Iver AK, Khaled G, Fang J, Maeda H. Exploiting the enhanced permeability and retention effect for tumor targeting. Drug Discov Today 2006;11:812–8.
[6] Lee CC, MacKay JA, Frechet JM, Szoka FC. Designing dendrimers for biological applications. Nat Biotechnol 2005;12:1517–26.
[7] Dvorak M, Kopeckova P, Kopecek J. High-molecular weight HPMA copolymer–adriamycin conjugates. J Control Release 1999;60:321–32.
[8] Takakura Y, Mahato RI, Nishikawa M, Hashida M. Control of pharmacokinetic profiles of drug–macromolecule conjugates. Adv Drug Deliv Rev 1996;19:377–99.
[9] Hespe W, Meier AM, Blankwater YJ. Excretion and distribution studies in rats with two forms of ^{14}Carbon labelled polyvinylpyrrolidone with a relatively low mean molecular weight after intravenous administration. Arzneimittelforschung 1977;27:1158–62.

[10] Gillies ER, Frechet JM. Dendrimers and dendritic polymers in drug delivery. Drug Discov Today 2005;10:35–43.
[11] Lee CC, Gillies ER, Fox ME, Guillaudeu SJ, Frechet JM, Dy EE, et al. A single dose of doxorubicin-functionalized bow-tie dendrimer cures mice bearing C-26 colon carcinomas. Proc Natl Acad Sci U S A 2006;103: 16649–54.
[12] Gillies ER, Dy E, Frechet JMJ, Szoka FC. Biological evaluation of polyester dendrimer: poly(ethylene oxide) "bow-tie" hybrids with tunable molecular weight and architecture. Mol Pharm 2005;2: 129–38.
[13] Kojima C, Kono K, Maruyama K, Takagishi T. Synthesis of polyamidoamine dendrimers having poly(ethylene glycol) grafts and their ability to encapsulate anticancer drugs. Bioconjug Chem 2000;11:910–7.
[14] Etrych T, Jelinkova M, Rihova B, Ulbrich K. New HPMA copolymers containing doxorubicin bound via pH-sensitive linkage: synthesis and preliminary in vitro and in vivo biological properties. J Control Release 2001;73:89–102.
[15] Ulbrich K, Subr V. Polymeric anticancer drugs with pH-controlled activation. Adv Drug Deliv Rev 2004;56:1023–50.
[16] Malik N, Evagorou EG, Dunkan R. Dendrimer–platinate: a novel approach to cancer chemotherapy. Anticancer Drugs 1999;10:767–76.
[17] Wiwattanapatapee R, Lomlim L, Saramunee K. Dendrimers conjugates for colonic delivery of 5-aminosalicylic acid. J Control Release 2003; 88:1–9.
[18] Kono K, Liu M, Frechet JMJ. Design of dendritic macromolecules containing folate or methotrexate residues. Bioconjug Chem 1999;10: 1115–21.
[19] Thomas TP, Majoros IJ, Kotlyar A, Kukowska-Latallo JF, Bielinska A, Myc A, et al. Targeting and inhibition of cell growth by an engineered dendritic nanodevice. J Med Chem 2005;48:3729–35.
[20] Greenwald RB, Conover CD, Choe YH. Poly(ethylene glycol) conjugated drugs and prodrugs: a comprehensive review. Crit Rev Ther Drug Carrier Syst 2000;17:101–61.
[21] Ihre HR, De Jesus OLP, Szoka FC, Frechet JMJ. Polyester dendritic systems for drug delivery applications: design, synthesis and characterization. Bioconjug Chem 2002;13:443–52.
[22] Gillies ER, Frechet JMJ. Designing macromolecules for therapeutic applications: polyester dendrimer–poly(ethylene oxide) "bow-tie" hybrids with tunable molecular weight and architecture. J Am Chem Soc 2002;124:14137–46.
[23] De Jesus OLP, Ihre HR, Gagne L, Frechet JM, Szoka FC. Polyester dendritic systems for drug delivery applications: in vitro and in vivo evaluation. Bioconjug Chem 2002;13:453–61.
[24] Kojima C, Toi Y, Harada A, Kono K. Preparation of poly(ethylene glycol)-attached dendrimers encapsulating photosensitizers for application to photodynamic therapy. Bioconjug Chem 2007;18:663–70.
[25] Haba Y, Harada A, Takagishi T, Kono K. Synthesis of biocompatible dendrimers with a peripheral network formed by linking of polymerizable groups. Polymer 2005;46:1813–20.
[26] Tomalia DA, Baker H, Dewald J, Hall M, Kallos G, Martin S, et al. A new class of polymers: starburst–dendritic macromolecules. Polymer J 1985;17:117–32.
[27] Takahashi T, Kono K, Itoh T, Emi N, Takagishi T. Synthesis of novel cationic lipids having polyamidoamine dendrons and their transfection activity. Bioconjug Chem 2003;14:764–73.
[28] Kono K, Akiyama H, Takahashi T, Takagishi T, Harada A. Transfection activity of polyamidoamine dendrimers having hydrophobic amino acid residues in the periphery. Bioconjug Chem 2005;16:208–14.
[29] Kiura K, Ohnoshi T, Tabata M, Shibayama T, Kimura I. Establishment of adriamycin-resistant subline of human small cell lung cancer showing multifactorial mechanism of resistance. Acta Med Okayama 1993;47: 191–7.
[30] Etrych T, Chytil P, Jelínková M, Říhová B, Ulbrich K. Synthesis of HPMA copolymers containing doxorubicin bound via a hydrazone linkage. Effect of spacer on drug release and in vitro cytotoxicity. Macromol Biosci 2002;2:43–52.
[31] Taatjes D, Koch TH. Nuclear targeting and retention of anthracycline antitumor drugs in sensitive and resistant tumor cells. Curr Med Chem 2001;8:15–29.
[32] Dufes C, Uchegbu IF, Schatzlein AG. Dendrimers in gene delivery. Adv Drug Deliv Rev 2005;57:2177–202.
[33] Allen TD, Cronshaw JM, Bagley S, Kiseleva E, Goldberg MW. The nuclear pore complex: mediator of translocation between nucleus and cytoplasm. J Cell Sci 2000;113:1651–9.
[34] Tsuruo T. Mechanisms of multidrug resistance and implications for therapy. Jpn J Cancer Res (Gann) 1988;79:285–96.
[35] Gerlach JH, Endicott JA, Juranka PF, Henderson G, Sarangi F, Deuchars KL, et al. Homolog between p-glycoprotein and a bacterial haemolysin transport protein suggests a model for multidrug resistance. Nature 1986;324:485–9.
[36] Minko T, Kopeckova P, Pozharov V, Kopecek J. HPMA copolymer bound adriamycin overcomes MDR1 gene encoded resistance in a human ovarian carcinoma cell line. J Control Release 1998;54:223–33.
[37] Minko T, Kopeckova P, Kopecek J. Comparison of the anticancer effect of free and HPMA copolymer-bound adriamycin in human ovarian carcinoma cells. Pharm Res 1999;16:986–96.
[38] Ryser HJP, Shen WC. Conjugation of methotrexate to poly(L-lysine) increases drug transport and overcomes drug resistance in cultured cells. Proc Natl Acad Sci U S A 1978;75:3867–70.
[39] Gurdag S, Khandare J, Stapels S, Mathely LH, Kannan RM. Activity of dendrimer–methotrexate conjugates on methotrexate-sensitive and resistant cell lines. Bioconjug Chem 2006;17:275–83.
[40] Yokoyama M, Okano T, Sakurai Y, Ekimoto H, Shibazaki C, Kataoka K. Toxicity and antitumor activity against solid tumors of micelle-forming polymeric anticancer drug and its extremely long circulation in blood. Cancer Res 1991;51:3229–36.
[41] Matsumura Y. Preclinical and clinical studies of anticancer drug-incorporated polymeric micelles. J Drug Target 2007;15:507–17.
[42] Nishiyama N, Okazaki S, Cabral H, Miyamoto M, Kato Y, Sugiyama Y, et al. Novel cisplatin-incorporated polymeric micelles can eradicate solid tumors in mice. Cancer Res 2003;63:8977–83.
[43] Bae Y, Fukushima S, Harada A, Kataoka K. Design of environment-sensitive supramolecular assemblies for intracellular drug delivery: polymeric micelles that are responsive to intracellular pH change. Angew Chem Int Ed 2003;42:4640–3.
[44] Bae Y, Nishiyama N, Fukushima S, Koyama H, Yasuhiro M, Kataoka K. Preparation and biological characterization of polymeric micelle drug carriers with intracellular pH-triggered drug release property: tumor permeability, controlled subcellular drug distribution, and enhanced in vivo antitumor efficacy. Bioconjug Chem 2005;16:122–30.

TECHNICAL NOTES

Synthesis and Characterization of Hyperbranched Poly(glycidol) Modified with pH- and Temperature-Sensitive Groups

Chie Kojima,[§,†] Kohei Yoshimura,[†] Atsushi Harada,[†] Yuichi Sakanishi,[‡] and Kenji Kono*[,†]

Department of Applied Chemistry, Graduate School of Engineering, Osaka Prefecture University, Osaka, Japan, and Daicel Chemical Industries, Ltd., Osaka, Japan. Received January 15, 2009; Revised Manuscript Received March 3, 2009

Hyperbranched poly(glycidol)s with varying degrees of polymerization were modified by reaction with succinic anhydride and isopropylamine to obtain novel pH- and thermosensitive polymers. These polymers exhibited phase transitions in response to decreasing pH and/or increasing temperature, depending on the degree of polymerization and the ratio of succinyl group to *N*-isopropylamide. It was possible to harvest a bioactive molecule, rose bengal, from solution using the phase transition of thermosensitive hyperbranched poly(glycidol).

INTRODUCTION

Dendrimers and hyperbranched polymers have three-dimensional structures and unique properties that are different from those of linear polymers (*1, 2*). For example, various types of dendrimers have been shown to be capable of encapsulating guest molecules, and many researchers have investigated their potential as carriers of bioactive molecules (*3*−*5*). Despite the lower regularity of their branched backbone structures, hyperbranched polymers tend to have spherical structures and exhibit properties in common with dendrimers. In addition, hyperbranched polymers tend to be more easily prepared than dendrimers (*6*−*8*). Thus hyperbranched polymers may be more useful, from a practical viewpoint, than dendrimers. To increase the usefulness of hyperbranched polymers, it is crucial to impart desired functionality to target hyperbranched polymers with appropriate structure and properties. However, there have been only a few reports on the modification of hyperbranched polymers with functional groups (*9, 10*).

Stimuli-sensitive properties are among the most useful functions of polymers for various fields of application. In particular, temperature- and pH-responsiveness are of great importance for biomedical applications. The temperature of target sites, such as tumor tissues, in the body can be changed safely by hyperthermia. Also, it is known that some cellular compartments and tissues have lower pH environments than normal physiological pH. For those reasons many efforts have been made to develop polymers with temperature-sensitive and pH-sensitive properties for biomedical use (*11*−*15*).

To increase the potential usefulness of hyperbranched polymers in the biomedical and related fields, in the present study we have attempted to render biocompatible hyperbranched polymers sensitive to temperature and pH. We propose a novel method for imparting thermosensitivity to temperature-insensitive polymers, by which side-chain units of thermosensitive polymers are introduced to the target polymer as temperature-sensitive moieties. We have previously reported that temperature-insensitive poly(amidoamine) and poly(propyleneimine) dendrimers can exhibit lower critical solution temperatures in aqueous solution after incorporation of isobutylamide or *N*-isopropylamide in their chain terminal groups (*16*−*19*). In the present study, we have applied this method to biocompatible hyperbranched poly(glycidol) (HPG) and examined the effectiveness of the method for the temperature sensitization (*20*). We have also attempted to impart pH sensitivity to HPG by the introduction of carboxyl groups. We have succeeded in making biocompatible hyperbranched polymers that respond to temperature and pH in ranges around normal physiological conditions, by controlling the relative proportions of the temperature-sensitive and pH-sensitive units.

MATERIALS AND METHODS

Materials and General Characterization. HPG with DP 10, 20, and 40 (HPG10, HPG20 and HPG40) were provided by Daicel Chemical Industries, Ltd. (Osaka, Japan). Succinic anhydride and pyridine were purchased from Kishida Chemical (Osaka, Japan). Triethylamine (TEA) was purchased from Sigma-Aldrich Corp. (St. Louis, MO). Isopropylamine (IPA) and rose bengal (RB) were purchased from Wako Pure Chemical Industries Ltd. (Osaka, Japan), 2-(1*H*-benzotriazol-1-yl)-1,1,3,3-tetramethyluronium hexafluorophosphate (HBTU) was obtained from Watanabe Chemical Industries, Ltd. (Hiroshima, Japan). ^{1}H NMR spectra were recorded using a JEOL JNM-LA400 instrument (JEOL, Japan).

Synthesis of Succinylated Hyperbranched Poly(glycidol)-(Suc-HPG). HPG10 (5.7 g, 7.5 mmol), HPG20 (5.8 g, 3.9 mmol), or HPG40 (5.9 g, 2.0 mmol) was dissolved in pyridine (60 mL). Twenty-five grams (2.6 × 10^2 mmol) of succinic anhydride was added, and the solution was stirred at 60−65 °C for 7 h under argon in the dark. The reaction mixtures were filtered to remove the solid deposit and concentrated by evaporation. The precipitates produced by addition of diethyl ether were purified on a Sephadex LH-20 column (GE health-

* To whom correspondence should be addressed. Tel.: +81 72 254 9330; fax: +81 72 254 9330; e-mail: kono@chem.osakafu-u.ac.jp.
† Osaka Prefecture University.
‡ Daicel Chemical Industries, Ltd.
§ Present affiliation: Nanoscience and Nanotechnology Research Center, Research Institutes for the Twenty First Century, Osaka Prefecture University, Japan.

10.1021/bc900016x CCC: $40.75
Published on Web 04/24/2009

Table 1. Synthesis Conditions, Yields, and Characterization of Various NIPAM-Suc-HPGs

	Suc-HPG							characterization by ^{1}H NMR		
									ratio in succinylation	
trial	DP	in feed [g(mmol)]	Et_3N (mmol)	HBTU (mmol)	IPA (nmol)	IPA equiv[a]	yield[(g%)]	succinilation(%)	-NIPAM	-COOH
1	10	0.94 (0.51)	15	7.11	15.20	2.5	0.88 (78)	87	0.96	0.04
2	10	1.19 (0.64)	19	4.16	3.20	0.4	1.02 (79)	91	0.37	0.63
3	20	1.00 (0.28)	18	11.86	11.78	1.9	0.97 (82)	91	0.94	0.06
4	20	1.01 (0.28)	18	7.14	9.14	0.8	1.04 (91)	88	0.79	0.21
5	20	1.22 (0.34)	20	6.38	4.79	0.6	1.18 (86)	94	0.60	0.40
6	20	1.23 (0.33)	19	3.21	3.21	0.4	1.02 (77)	97	0.34	0.66
7	40	1.02 (0.14)	17	8.18	9.30	1.6	1.14 (93)	95	0.96	0.04
8	40	1.09 (0.15)	26	8.28	5.09	0.8	1.12 (92)	98	0.80	0.20
9	40	1.24 (0.17)	21	6.91	5.18	0.7	1.27 (92)	95	0.60	0.40
10	40	1.26 (0.18)	21	3.35	3.35	0.4	1.20 (89)	98	0.33	0.67

[a] Per terminal group.

Scheme 1

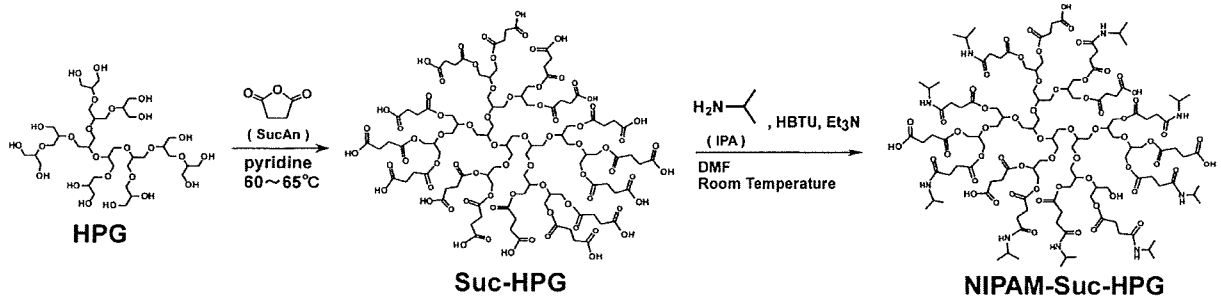

care) by elution with methanol to obtain Suc-HPG10, Suc-HPG20, and Suc-HPG40 with yields 5.2 g (37%), 8.3 g (59%), and 10.3 g (74%), respectively.

δ_H (Suc-HPG, 400 MHz, CD_3OD): 2.6 (br, $OCOCH_2C$-H_2COOH), 3.4−4.1 (br, HPG-scaffold), 4.1−4.5 (br, CH_2OCO), 5.0−5.3 (br, >CHOCO).

Synthesis of *N*-Isopropylamination of Succinylated Hyperbranched Poly(glycidol) (NIPAM-Suc-HPG). Suc-HPG10, Suc-HPG20, and Suc-HPG40 were dispersed in water and evaporated. This treatment was repeated four times, and then the residues were lyophilized to completely remove methanol. The methanol-free Suc-HPG10, Suc-HPG20, and Suc-HPG40 were reacted with isopropylamine at different ratios (see reaction conditions given in Table 1). Because HBTU is an effective condensation reagent that can form ester bonds, it is necessary to take care to avoid contamination and addition of alcohol. In a typical preparation Suc-HPG20 was dissolved in distilled DMF (13 mL), triethylamine and HBTU were added, IPA diluted with distilled DMF (2.32 M) was added, and the mixture was stirred at 28−30 °C for 3 days under argon in the dark. After evaporation of the reaction mixture, the residue was purified by reprecipitation from acetic acid−1 N HCl and washed several times with diethyl ether. The crude product, dispersed in acetic buffer (pH 4−5) to adjust pH, was purified on a Sephadex LH-20 column (GE Healthcare) by elution with methanol. Other polymers were synthesized by varying the amounts of each material according to Table 1. The yields of the synthesized polymers are given in Table 1.

δ_H (400 MHz, CD_3OD): δ 1.1 (d, $NHCH(CH_3)_2$), 2.5 (br, $OCOCH_2CH_2CONH$-), 2.6 (br, $OCOCH_2CH_2COOH$ and $OCOCH_2CH_2CONH$), 3.4−4.1 (br, HPG-scaffold), 3.9 (br, $COONHCH(CH_3)_2$), 4.1−4.5 (br, CH_2OCO), 5.0−5.3 (br, >CHOCO), 7.8 (br, CONH).

Measurement of Phase Transition. The turbidity of solutions of NIPAM-Suc-HPGs in 10 mM phosphate containing 150 mM NaCl buffer, pH 5.0−7.4, was measured at 700 nm using a Jasco Model V-560 spectrophotometer equipped with a Peltier type thermostatic cell holder coupled with an ETC-505T controller. The heating rate of the sample cell was maintained at 1.0 °C min^{-1}. The cloud points were taken as the initial break points in the resulting transmittance versus temperature curves.

Temperature-Dependent Separation of Rose Bengal. A solution of rose bengal (59 μM) containing NIPAM-Suc-HPG40 (5 mg mL^{-1}, 0.59 mM) or unmodified HPG40 (5 mg mL^{-1}, 1.7 mM) in phosphate buffer (10 mM phosphate containing 150 mM NaCl buffer, pH 7.4) was prepared. After 30 min incubation at 4 or 40 °C, the solution was centrifuged at 15 000 rpm for 30 min at 4 or 40 °C. The supernatants of rose bengal solutions without polymer were also prepared. The absorption spectra of the supernatants were obtained using a Jasco Model V-560 spectrophotometer equipped with a thermomodule (ETC-717T, Jasco Inc., Japan).

RESULTS AND DISCUSSION

Synthesis of NIPAM-Suc-HPGs. Stimuli-responsive polymers based on HPG were synthesized according to Scheme 1. HPGs with degree of polymerization (DP) 10, 20, and 40 were reacted with excess succinic anhydride to provide a pH sensitive unit for HPG (Suc-HPG). Suc-HPGs were then reacted with different amounts of isopropylamine. The experimental conditions for the polymers that were synthesized are shown in Table 1. The synthesized compounds were characterized by ^{1}H NMR. The NMR spectra of unmodified HPG20, Suc-HPG20, and NIPAM-Suc-HPG20 (#5) are shown in Figure 1. The spectrum of Suc-HPG20 reveals signals derived from HPG (3.4−4.0 ppm) and the succinyl unit (2.6 ppm). The signals at 5.0−5.3 ppm and 4.1−4.5 ppm were shifted from 3.4−4.0 ppm by making ester bonds in HPG20 (methine and methylene, respectively). The integral ratio of the succinyl unit signal (2.6 ppm) to the HPG20 signals (3.4−4.1, 4.1−4.5, and 5.0−5.3 ppm) indicates that virtually all terminal hydroxyl groups of HPG20 were succinylated. The same results were obtained for HPG10 and HPG40. The spectrum of NIPAM-Suc-HPG20 (#5) is shown in Figure 1C. Signals from the NIPAM unit (1.1 and 3.9 ppm) were observed in addition to the Suc-HPG signals. The signals

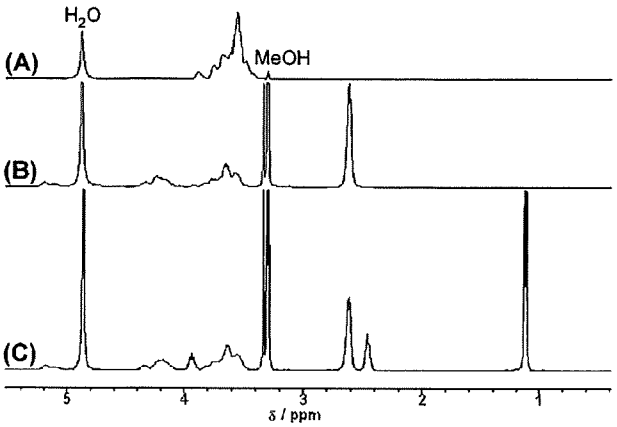

Figure 1. ^{1}H NMR spectra of HPG20 (A), Suc-HPG20 (B), and NIPAM-Suc-HPG20 (#5) (C) in CD_3OD.

at 2.6 ppm were shifted to 2.5 ppm by making amide bonds in Suc-HPG20. From the integral ratios of the succinyl and NIPAM unit signals to the HPG20 signals, we estimated the proportions of NIPAM and Suc in HPG. The results for all of the polymers that were synthesized are shown in Table 1. We found that the extent of succinylation slightly decreased after amidation with isopropylamine. This might be caused by the hydrolysis of ester bonds in the second reaction step and purification. We synthesized polymers with different DPs and with varying proportions of NIPAM groups and unreacted carboxyl groups.

Phase Transitions of NIPAM-Suc-HPGs. The phase transition of aqueous solutions containing the synthesized polymers was examined. We could not observe a phase transition for unmodified HPGs and Suc-HPGs in 10 mM phosphate buffer containing 150 mM sodium chloride (pH 5.0−7.4). However, NIPAM-Suc-HPGs exhibited thermosensitive behavior depending on the conditions of preparation. We examined first the influence of the DP on the thermosensitivity of the polymers. Figure 2A shows the optical transmittance of aqueous solutions (pH 5.0) of $NIPAM_{0.96}$-Suc-HPG10, $NIPAM_{0.94}$-Suc-HPG20, and $NIPAM_{0.96}$-Suc-HPG40, in which almost all of the hydroxy groups were replaced by NIPAM groups. The transmittance changed drastically at 16, 10, and 7 °C which are called cloud points. The decrease of cloud point with increasing DP of the HPG polymers is consistent with previously reported observations (*9*). It is thought that increase of the terminal group density and van der Waals interaction might result in the lower cloud point of polymer with higher DP. These cloud points are lower than the LCST of polyNIPAM (32 °C). The lower cloud point may be caused by the different structure of the polymer and hydrogen bonds between the main chain and the side chain of the polymer.

We also investigated the influence of the relative proportions of NIPAM groups and unreacted carboxyl groups on the thermosensitivity of the polymers. Figure 2B shows that the optical transmittance of aqueous solutions (pH 5.0) of $NIPAM_{0.94}$-Suc-HPG20, $NIPAM_{0.79}$-Suc-HPG20, and $NIPAM_{0.60}$-Suc-HPG20 drastically changed at 10, 13, and 25 °C, respectively, but that of $NIPAM_{0.33}$-Suc-HPG20 did not. Similar behavior was observed for solutions of a series of HPG40-based polymers (see Supporting Information), indicating that a larger proportion of NIPAM groups induced the phase transition because of the enhanced hydrophobicity.

Because the unreacted carboxyl groups of the NIPAM-Suc-HPG can act as a pH sensor, we investigated the influence of pH on the thermosensitivity of the polymers. The cloud points of $NIPAM_{0.60}$-Suc-HPG20 at pH 5.0, 5.2, and 5.4 were 28, 38, and 56 °C (Figure 2C), respectively, and a cloud point was not

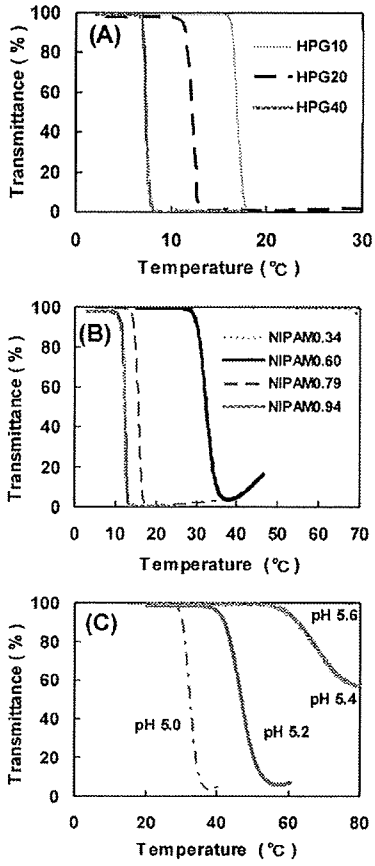

Figure 2. pH- and temperature sensitivity of various NIPAM-Suc-HPGs. (A) The influence of the DP of HPG on the thermosensitivity. Temperature dependence of transmittance for solutions of $NIPAM_{0.96}$-Suc-HPG10, $NIPAM_{0.94}$-Suc-HPG20, and $NIPAM_{0.96}$-Suc-HPG20 at pH 5.0. (B) The influence of the proportion of NIPAM on the thermosensitivity. Temperature dependence of transmittance for solutions of $NIPAM_{0.34}$-Suc-HPG20, $NIPAM_{0.60}$-Suc-HPG20, $NIPAM_{0.79}$-Suc-HPG20, and $NIPAM_{0.94}$-Suc-HPG20 at pH 5.0. (C) pH-sensitivity of $NIPAM_{0.60}$-Suc-HPG20. Temperature dependence of transmittance for solutions of $NIPAM_{0.60}$-Suc-HPG20 at pH 5.0, 5.2, 5.4, and 5.6.

detected at pH 5.6. Similar behavior was observed for solutions of a series of HPG40-based polymers (see Supporting Information). Since $NIPAM_{0.60}$-Suc-HPG20 contained 40% carboxyl group and 60% NIPAM group, this polymer was responsive to both pH and temperature, as we expected. Protonated carboxyl groups at lower pH may increase the hydrophobicity and induce hydrogen bond formation, leading to lower cloud point. The cloud points of $NIPAM_{0.94}$-Suc-HPG20 at pH 5.0 and 7.4 were the same temperature (see Supporting Information). Because this polymer contained few remaining carboxyl groups, it was not sensitive to pH. Consequently, polymers containing an appropriate amount of carboxyl groups can sense both pH and temperature, and it is possible to control pH- and thermosensitivity by tuning the DP, and the relative proportions of NIPAM and carboxyl groups.

Temperature-Dependent Separation of Rose Bengal by Using NIPAM-Suc-HPGs. Thermosensitive dendrimers can act as a nanocapsule for harvesting bioactive molecules (*5*). We investigated the temperature-dependent encapsulation ability of NIPAM-Suc-HPG to rose bengal (RB), which is a type of photosensitizer (*4, 21*). RB aqueous solution with and without NIPAM-Suc-HPG were prepared and heated to 40 °C. After centrifugation, the UV−vis spectra of the solutions were obtained. As shown in Figure 3, the absorption spectrum of RB in the presence of NIPAM-Suc-HPG almost disappeared after

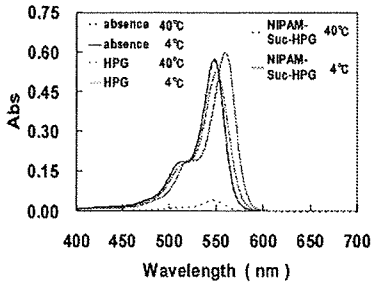

Figure 3. UV−vis spectra of RB in the absence (black) and the presence (red) of $NIPAM_{0.96}$-Suc-HPG40 at 4 °C (solid lines) and 40 °C (dotted lines). The spectrum in the presence of unmodified HPG40 (blue) is also shown.

heating, although the spectrum in the absence of NIPAM-Suc-HPG was unchanged. The spectrum at 40 °C in the presence of HPG, which is not thermosensitive, was the same as at 4 °C. Thus the thermosensitive hyperbranched polymer is a candidate as a temperature-dependent carrier of bioactive molecules. This property is of benefit for accumulation of drug molecules at the site of heated tissue.

In conclusion, we synthesized and characterized NIPAM-Suc-HPG, which contained both carboxyl groups as pH-sensing units and NIPAM groups as thermosensitive units. The pH- and thermosensitivity is dependent on the DP of based polymers and the relative proportions of pH- and thermosensing units. The pH- and thermosensitivity of the polymer can thus be adjusted and controlled by selecting the DP and tuning the reaction conditions. Shen et al. reported very recently a preparation of a type of thermosensitive HPG, by modification of *N*-isopropylacrylamide after the substitution of hydroxyl groups by amino groups. This polymer was sensitive to pH and temperature due to the tertiary amino groups and the NIPAM groups (*9*). However, the pH range of pH sensitivity was above pH 7, which is unlikely to occur in the body. By contrast, our polymers responded in the range from pH 5 to 7, a typical physiological pH range, and a photosensitizer, rose bengal, can be harvested by adding these polymers and heating. Consequently, NIPAM-Suc-HPG is a candidate as a functional material for biomedical applications.

ACKNOWLEDGMENT

We are grateful to Daicel Chemical Industries, Ltd. (Osaka, Japan) for the kind gift of HPGs and for financial support.

Supporting Information Available: Figures S1–S3. This material is available free of charge via the Internet at http://pubs.acs.org.

LITERATURE CITED

(1) Lee, C. C., MacKay, J. A., Frechet, J. M. J., and Szoka, F. C. (2005) Designing dendrimers for biological applications. *Nat. Biotechnol. 12*, 1517–1526.

(2) Boas, U., and Heegaad, P. M. H. (2004) Dendrimers in drug research. *Chem. Soc. Rev. 33*, 43–63.

(3) Kojima, C., Kono, K., Maruyama, K., and Takagishi, T. (2000) Synthesis of polyamidoamine dendrimers having poly(ethylene glycol) grafts and their ability to encapsulate anticancer drugs. *Bioconjugate Chem. 33*, 9169–9172.

(4) Kojima, C., Toi, Y., Harada, A., and Kono, K. (2007) Preparation of polyethylene glycol-attached dendrimers encapsulating photosensitizers for application to photodynamic therapy. *Bioconjugate Chem. 18*, 663–670.

(5) Kono, K., Miyoshi, T., Haba, Y., Murakami, E., Kojima, C., and Harada, A. (2004) Temperature sensitivity control of alkylamide-terminated poly(amidoamine) dendrimers induced by guest molecule binding. *J. Am. Chem. Soc. 129*, 7222–7223.

(6) Sunder, A., Mulhaupt, R., Haag, R., and Frey, H. (2000) Hyperbranched polyether polyols: a modular approach to complex polymer architectures. *Adv. Mater. 12*, 235–239.

(7) Sunder, A., Heinemann, J., and Frey, H. (2000) Controlling the growth of polymer trees: concepts nad perspectives for hyperbrnached polymers. *Chem.—Eur. J. 6*, 2499–2506.

(8) Frey, H., and Haag, R. (2002) Dendritic polyglycerol: a new versatile biocompatible material. *Rev. Mol. Biotechnol. 90*, 257–267.

(9) Shen, Y., Kuang, M., Shen, Z., Nieberle, J., Duan, H., and Frey, H. (2008) Gold nanoparticles coated with a thermosensitive hyperbranched polyelectrolyte: towards smart temperature and pH nanosensors. *Angew. Chem., Int. Ed. 47*, 2227–2230.

(10) Liu, H., Chen, Y., and Shen, Z. (2007) Thermoresponsive hyperbranched polyethylenimines with isobutyramide functional groups. *J. Polym. Sci., Part A 45*, 1177–1184.

(11) Rijcken, C. J. F., Soga, O., Hennink, W. E., and van Nostrum, C. F. J. (2007) Triggered destabilisation of polymeric micelles and vesicles by changing polymers polarity: An attractive tool for drug delivery. *Controlled Release 120*, 131–148.

(12) Alarcon, C. H., Pennadam, S., and Alexander, C. (2005) Stimuli responsive polymers for biomedical applications. *Chem. Soc. Rev. 34*, 276–285.

(13) Schmaljohann, D. (2006) Thermo- and pH-responsive polymers in drug delivery. *Adv. Drug Delivery Rev. 58*, 1655–1670.

(14) Kono, K., Zenitani, K., and Takagishi, T. (1994) Novel pH-sensitive liposomes: liposomes bearing a poly(ethylene glycol) derivative with carboxyl groups. *Biochim. Biophys. Acta 1193*, 1–9.

(15) Sakaguchi, N., Kojima, C., Harada, A., and Kono, K. (2008) Preparation of pH-sensitive poly(glycidol) derivatives with varying hydrophobicities: their ability to sensitize stable liposomes to pH. *Bioconjugate Chem. 19*, 1040–1048.

(16) Haba, Y., Harada, A., Takagishi, T., and Kono, K. (2004) Rendering poly(amidoamine) or poly(propylenimine) dendrimers temperature sensitive. *J. Am. Chem. Soc. 126*, 12760–12761.

(17) Haba, Y., Kojima, C., Harada, A., and Kono, K. (2006) Control of temperature-sensitive properties of poly(amidoamine) dendrimers using peripheral modification with various alkylamide groups. *Macromolecules 39*, 7451–7453.

(18) Tono, Y., Kojima, C., Haba, Y., Takahashi, T., Harada, A., Yagi, S., and Kono, K. (2006) Thermosensitive properties of poly (amidoamine) dendrimers with peripheral phenylalanine residues. *Langmuir 22*, 4920–4922.

(19) Haba, Y., Kojima, C., Harada, A., and Kono, K. (2007) Comparison of thermosensitive properties between poly(amidoamine) dendrimers having peripheral N-isopropylamide groups and linear polymers with the same groups. *Angew. Chem., Int. Ed. 46*, 234–237.

(20) Kainthan, R. K., Janzen, J., Levin, E., Devine, D. V., and Brooks, D. E. (2006) Biocompatibility testing of branched and linear polyglycidol. *Biomacromolecules 7*, 703–709.

(21) Detty, M. R., Gibson, S. L., and Wagner, S. J. (2004) Current clinical and preclinical photosensitizers for use in photodynamic therapy. *J. Med. Chem. 47*, 3897–3915.

BC900016X

ARTICLE IN PRESS
COREL-05399; No of Pages 9
Journal of Controlled Release xxx (2010) xxx–xxx
Contents lists available at ScienceDirect
Journal of Controlled Release
journal homepage: www.elsevier.com/locate/jconrel
NANOMEDICINE

Carboxylated hyperbranched poly(glycidol)s for preparation of pH-sensitive liposomes

Eiji Yuba [a], Atsushi Harada [a], Yuichi Sakanishi [b], Kenji Kono [a,*]

[a] Department of Applied Chemistry, Graduate School of Engineering, Osaka Prefecture University, 1-1 Gakuen-cho, Naka-ku, Sakai, Osaka 599-8531, Japan
[b] Daicel Chemical Industry, Ltd., 2-1-4, Higashisakae, Ohtake, Hiroshima 739-0695, Japan

ARTICLE INFO

Article history:
Received 19 November 2009
Accepted 1 March 2010
Available online xxxx

Keywords:
pH-sensitive liposome
Cytoplasmic delivery
Hyperbranched polymer
Membrane fusion
Dendritic cell

ABSTRACT

Previous reports by the authors described intracellular delivery using liposomes modified with various carboxylated poly(glycidol) derivatives. These linear polymer-modified liposomes exhibited a pH-dependent membrane fusion behavior in cellular acidic compartments. However, the effect of the backbone structure on membrane fusion activity remains unknown. Therefore, this study specifically investigated the backbone structure to obtain pH-sensitive polymers with much higher fusogenic activity and to reveal the effect of the polymer backbone structure on the interaction with the membrane. Hyperbranched poly(glycidol) (HPG) derivatives were prepared as a new type of pH-sensitive polymer and used for the modification of liposomes. The resultant HPG derivatives exhibited high hydrophobicity and intensive interaction with the membrane concomitantly with the increasing degree of polymerization (DP). Furthermore, HPG derivatives showed a stronger interaction with the membrane than the linear polymers show. Liposomes modified with HPG derivatives of high DP delivered contents into the cytosol of DC2.4 cells, a dendritic cell line, more effectively than the linear polymer-modified liposomes do. Results show that the backbone structure of pH-sensitive polymers affected their pH-sensitivity and interaction with liposomal and cellular membranes.

1. Introduction

Cytoplasmic delivery of bioactive molecules such as proteins and nucleic acids, which are unable to permeate a cellular membrane themselves, is important to establish therapies—such as immunotherapy and gene therapy—based on these molecules. Although various systems have been attempted for application to cytoplasmic delivery, one of the promising systems is pH-sensitive liposome, which induces destabilized and/or fusogenic activity under mildly acidic conditions. Various methods have been applied to produce pH-sensitive liposomes. For example, pH-sensitive amphiphiles, such as oleic acid and cholesteryl hemisuccinate, have been mixed with non-bilayer-forming phospholipid dioleoyl phosphatidylethanolamine (DOPE) to yield pH-sensitive liposomes [1,2]. Another efficient method for pH-sensitization of liposome is the modification of stable liposomes with pH-sensitive membrane active molecules such as fusion peptides derived from viral fusogenic proteins, or synthetic polymers with carboxyl groups such as poly(alkyl acrylic acid)s [3,4]. Earlier studies by the authors developed a series of carboxylated poly(glycidol) derivatives for pH-sensitization of liposomes [5–7]. These polymers have a linear backbone structure similar to that of poly(ethylene glycol) (PEG) and carboxyl groups on the side chains, which control the interaction of the polymer backbone with lipid membranes in a pH-dependent manner. Earlier studies showed that these polymer-modified liposomes are stable at neutral pH, but that they exhibit considerable destabilization under mildly acidic conditions and deliver contents into cytosol by membrane fusion with endosome/lysosome membranes [5–7].

Generally, membrane fusion as a biological function is mediated by fusogenic proteins. For example, enveloped viruses of various kinds have proteins that promote fusion of their envelope with cellular membranes to invade target cells. A very well studied viral fusion protein is influenza virus hemagglutinin (HA), which forms a fusion-active trimeric structure in the intracellular acidic compartment endosome and causes membrane fusion [8]. Considering these protein-mediated fusion processes, it might be important that fusogenic proteins having a bulky steric structure interact with a membrane for efficient membrane fusion because such interaction might generate a defective area and initiate membrane fusion.

Synthetic polymers of various kinds reportedly interact with membranes and induce membrane fusion [4,5,7,9,10]. Considering that these synthetic polymers generally have a linear structure, it is presumed that their interaction with membranes might not be so effective to generate defective regions for initiation of membrane fusion as sterically bulky proteins do. To date, the influence of the backbone structure of fusogenic polymers on their membrane fusion activity remains unknown. Hyperbranched polymers tend to take on a three-dimensional and spherical structure, which differs from those of

* Corresponding author. Tel./fax: +81 722 54 9330.
E-mail address: kono@chem.osakafu-u.ac.jp (K. Kono).

0168-3659/$ – see front matter © 2010 Elsevier B.V. All rights reserved.
doi:10.1016/j.jconrel.2010.03.001

linear polymers taking on a random coil structure [11–15]. Recently, 3-methyl-glutarylated poly(glycidol) was synthesized by the authors. It destabilizes phospholipid membranes under a weakly acidic environment and causes membrane fusion [7]. For the present study, its analogous polymers were prepared using hyperbranched poly(glycidol)s (HPGs) with different degrees of polymerization (DP), 3-methyl-glutarylated HPGs (MGlu-HPGs). Results described herein demonstrate that the DP and backbone structure of the pH-sensitive polymers affected their pH-sensitive fusion properties and their performance as intracellular delivery vehicles.

2. Materials and methods

2.1. Materials

HPGs with DPs of 10, 20, 40 and 60, which are respectively designated as HPG10, HPG20, HPG40 and HPG60, were provided by Daicel Chemical Industries, Ltd. (Osaka, Japan). Egg yolk phosphatidylcholine (EYPC) and L-dioleoyl phosphatidylethanolamine (DOPE) were kindly donated by NOF Co. (Tokyo, Japan). Pyrene, pyranine, 1-aminodecane and Triton X-100 were obtained from Tokyo Chemical Industries Ltd. (Tokyo, Japan). *p*-Xylene-bis-pyridinium bromide (DPX) was from Molecular Probes (Oregon, USA). *N*-(7-nitrobenz-2-oxa-1,3-diazol-4-yl)dioleoyl phosphatidylethanolamine (NBD-PE) and lissamine rhodamine B-sulfonyl phosphatidylethanolamine (Rh-PE) were purchased from Avanti Polar Lipids (Birmingham, AL, USA). 3-Methylglutaric anhydride was obtained from Aldrich (Milwaukee, WI). 4-(4,6-Dimethoxy-1,3,5-triazin-2-yl)-4-methyl morpholinium chloride (DMT-MM) was from Wako Pure Chemical Industries Ltd. (Osaka, Japan). Ovalbumin (OVA) and fluorescein isothiocyanate (FITC) were purchased from Sigma (St. Louis, MO.). 3-Methyl-glutarylated linear poly(glycidol) (MGluPG) (Fig. 1) was prepared as previously reported using two kinds of poly(glycidol)s with different molecular weights: PG76 with number average molecular weight (Mn) of 5.6×10^3 and weight average molecular weight (Mw) of 8.7×10^3, and PG222 with Mn of 1.6×10^4 and Mw of 2.5×10^4, which were evaluated using gel permeation chromatography with Shodex KD-803 and KF805L columns (Showa Denko) and poly (ethylene glycol)s as the standard. Obtained polymers were designated as MGluPG76 and MGluPG222, respectively [7]. FITC–OVA was prepared by reacting OVA (10 mg) with FITC (11.8 mg) in 0.5 M $NaHCO_3$ (4 mL, pH 9) at 4 °C for three days and subsequent dialysis.

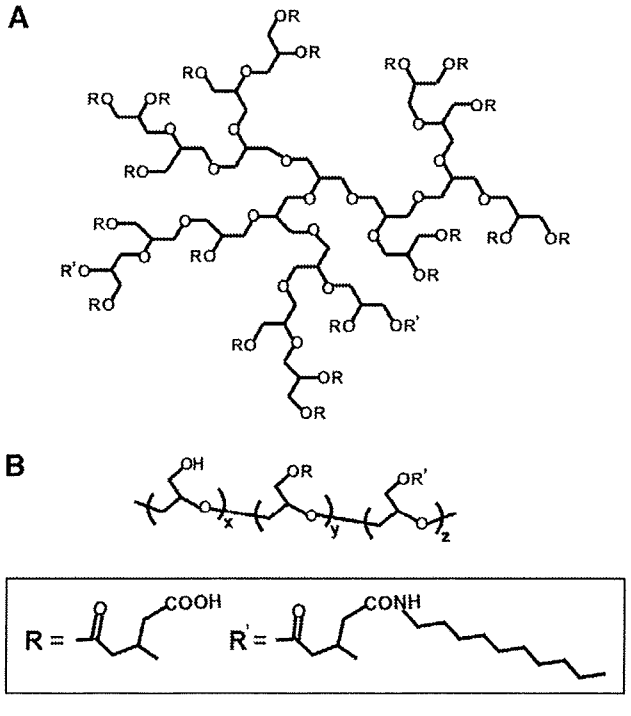

Fig. 1. Structures of MGlu-HPG20-C_{10} (A) and linear MGluPG-C_{10} (B).

2.2. Synthesis of hyperbranched poly(glycidol) derivatives

3-Methyl-glutarylated hyperbranched poly(glycidol) (MGlu-HPG) was prepared by reaction of HPG with varying DPs with 3-methylglutaric anhydride. HPG10 (0.765 g) and LiCl (0.765 g) were dissolved in pyridine (18 mL) and 3.0 equiv. of 3-methylglutaric anhydride (3.98 g) was added to the solution. The mixed solution was kept at 115 °C for 24 h with stirring. Then, the reaction mixture was evaporated and dialyzed against water for 3 days. The product was recovered by freeze-drying. HPG20, HPG40 and HPG60 were also reacted with 3-methylglutaric anhydride by the same procedure. As anchor moieties for fixation of MGlu-HPG onto liposome membranes, 1-aminodecane was combined with carboxyl groups of MGlu-HPG. Each polymer was dissolved in water around pH 7.4, and 1-aminodecane (0.18 equiv. to carboxyl group of polymer) was reacted to carboxyl groups of the polymer using DMT-MM (0.18 equiv. to carboxyl groups of polymers) at room temperature for three days with stirring. The obtained polymers were purified by dialysis in water.

2.3. Cell culture

DC2.4 cells, which were an immature murine dendritic cell (DC) line, were provided from Dr. K. L. Rock (Harvard Medical School, USA) and were grown in RPMI 1640 supplemented with 10% FBS (MP Biomedical, Inc.), 2 mM L-glutamine, 100 μM non-essential amino acids (Gibco, Inc.), 50 μM 2-mercaptoethanol (2-ME) and antibiotics at 37 °C [16].

2.4. Precipitation pH

Precipitation pH of polymers was determined by measuring the optical density of aqueous polymer solutions (0.25 mg/mL) at various pHs. Polymers were dissolved in 30 mM sodium acetate and 120 mM NaCl aqueous solution of various pHs. After 5 min-incubation at 25 °C, optical densities of the polymer solutions at 500 nm were measured by using a spectrophotometer (Jasco V-520). Precipitation pH was determined using optical density–pH profiles as the pH at which OD drastically rose.

2.5. Pyrene fluorescence

A given amount of pyrene in acetone solution was added to an empty flask, and acetone was removed under vacuum. Polymer (0.2 mg/mL) dissolving in 25 mM MES and 125 mM NaCl solution of a given pH was added to the flask, yielding 1 μM concentration of pyrene. The sample solution was stirred overnight at room temperature, and emission spectra with excitation at 337 nm were recorded. The fluorescence intensity ratio of the first band at 373 nm to the third band at 384 nm (I_1/I_3) was analyzed as a function of pH of the solution.

2.6. Preparation of pyranine-loaded liposomes

500 μL of aqueous 35 mM pyranine, 50 mM DPX, and 25 mM MES solution (pH 7.4) were added to a dry, thin membrane of EYPC (7 mg), and the mixture was sonicated for 2 min using a bath-type sonicator. The liposome suspension was further hydrated by freezing and thawing, and was extruded through a polycarbonate membrane with a pore size of 100 nm. The liposome suspension was applied to a

sepharose4B column to remove free pyranine from the pyranine-loaded liposomes. Polymer-modified liposomes were also prepared according to the above procedure using dry membranes of mixtures of EYPC and various polymers (EYPC/polymer = 7/3, w/w).

2.7. Release of pyranine from liposome

Release of pyranine from liposome was measured as previously reported [7,17]. Pyranine fluorescence was quenched by DPX inside of the liposomes, but this molecule exhibits intense fluorescence when released from the liposome [17]. For the study of the interaction of polymers with lipid membranes, a given amount of the polymer dissolved in the same buffer (final concentration: 0.013 mg/mL) at 25 °C was added to a suspension of pyranine-loaded liposomes (lipid concentration: 2.0×10^{-5} M) in 25 mM MES and 125 mM NaCl buffer of varying pHs,, and fluorescence intensity (512 nm) of the mixed suspension was followed with excitation at 416 nm using a spectrofluorometer (Jasco FP-6500). For the study of the release behavior of polymer-modified liposomes, polymer-modified liposomes encapsulating pyranine were added to 25 mM MES and 125 mM NaCl buffer of varying pHs at 37 °C and fluorescence intensity of the suspension was monitored (lipid concentration: 2.0×10^{-5} M). The percent release of pyranine from liposomes was defined as

$$\text{Release}(\%) = (F_t - F_i) / (F_f - F_i) \times 100$$

where F_i and F_t mean the initial and intermediary fluorescence intensities of the liposome suspension, respectively. F_f is the fluorescent intensity of the liposome suspension after the addition of TritonX-100 (final concentration: 0.1%).

2.8. Liposome size change

EYPC liposomes were prepared as described above without pyranine and DPX. EYPC liposomes (4.1 mM, 103.4 μL, pH 7.4) were added to 25 mM MES and 125 mM NaCl buffer of various pHs (2370 μL). And then, 26.6 μL of polymer solution of the same buffer (10 mg/mL, pH 7.4) was added. The mixed solutions were incubated overnight. pH of the mixed solution was measured and liposome diameters were evaluated using a Nicomp 380 ZLS dynamic light scattering instrument (Particle Sizing Systems, Santa Barbara, CA) equipped with a 35 mW laser (λ = 632.8 nm). Data were obtained as an average of more than three measurements on different samples.

2.9. Intracellular behavior of liposomes

The FITC–OVA-loaded liposomes containing Rh-PE were prepared as described above except that mixtures of polymers and EYPC containing Rh-PE (0.1 mol%) were dispersed in phosphate-buffered saline containing FITC–OVA (4 mg/mL). The DC2.4 cells (2×10^5 cells) cultured for 2 days in 35-mm glass-bottom dishes were washed with Hank's balanced salt solution (HBSS, Sigma), and then incubated in serum-free RPMI medium (500 μL). The FITC–OVA-loaded liposomes (100 μg/mL of FITC–OVA, 500 μL) were added gently to the cells and incubated for 4 h at 37 °C. After the incubation, the cells were washed with HBSS three times. Confocal laser scanning microscopic (CLSM) analysis of these cells was performed using LSM 5 EXCITER (Carl Zeiss Co. Ltd.). Fluorescence intensity of these cells was also determined using a Coulter Epics XL Flow Cytometer (Coulter Corporation, Florida, USA) [18].

2.10. Fusion of liposomes in cell

Liposomes containing NBD-PE and Rh-PE (each 0.6 mol%) were prepared as described above using DOPE as an additional lipid component and suspended in PBS. The DC2.4 cells (2×10^5 cells) cultured for 2 days in 35-mm glass-bottom dishes were washed with HBSS, and then incubated in serum-free RPMI medium (500 μL). Then, the liposome suspensions (1.0 mM of liposomal lipid, 500 μL) were added gently to the medium of the cells and incubated for 4 h at 37 °C. After the incubation, the cells were washed with HBSS three times and analyzed by CLSM. Fluorescence of NBD-PE and Rh-PE was observed through specific path filters (λ_{em} = 500–530 nm for NBD-PE and λ_{em} > 560 nm for Rh-PE) with excitation at 488 nm. Fluorescence intensities of these cells were also determined by flow cytometry with excitation at 488 nm. The fluorescence intensity ratio of NBD-PE to Rh-PE was defined as

$$\text{NBD / Rh} = (I_{NBD} - I_{NBD,0}) / (I_{Rh} - I_{Rh,0})$$

where I_{NBD} and I_{Rh} are the fluorescence intensities of the liposome-treated cells detected by FL1 (λ_{em} = 505–545 nm) and FL2 channel (λ_{em} = 560–590 nm), respectively. $I_{NBD,0}$ and $I_{Rh,0}$ are the fluorescence intensities of untreated cells detected by FL1 and FL2 channel, respectively.

3. Results and discussion

3.1. Characterization of HPG derivatives

Previous studies developed and assessed a series of carboxylated linear poly(glycidol) derivatives for pH-sensitization of liposome [5–7]. Especially, MGluPG-modified liposomes were stable at neutral pH and showed strong fusogenic activity under weakly acidic conditions [7]. Considering the function of viral fusogenic proteins for viral membrane fusion, it was assumed that a polymer with a three-dimensional backbone structure can interact with membranes more effectively and intensively than a linear polymer. Therefore, a hyperbranched polymer was selected as a backbone structure. We prepared four kinds of MGlu-HPGs with different molecular sizes, namely MGlu-HPG10, MGlu-HPG20, MGlu-HPG40, and MGlu-HPG60, using HPGs with DPs of 10, 20, 40, and 60, as pH-sensitive polymers with a hyperbranched structure. Also, two kinds of MGluPGs with different chain lengths, namely MGluPG76 and MGluPG222, were prepared as pH-sensitive polymers with a linear structure, using PG76 and PG222. Hydrodynamic diameters of HPG10, HPG20, HPG40, HPG60, PG76, and PG222 were estimated to be 2.0, 2.6, 3.2, 3.6, 4.8, and 8.6 nm, respectively, according to the method of Hester and Mitchell using GPC with PEG standards [19].

Compositions of these polymers, which were estimated using ^{1}H NMR, are presented in Table 1. For all polymers, only low percentages of unreacted glycidol units remained on the polymer backbone after the reaction of HPG with 3-methylglutaric anhydride, demonstrating the high efficiency of these reactions, which is consistent with a previous report [7]. Fundamentally, every repeating unit possesses a carboxyl group in the resultant polymers. Results of an earlier study showed that attachment of 1-aminodecane to about 8 unit% of a

Table 1
Compositions of various hyperbranched and linear poly(glycidol) derivatives.

Polymer	Hydroxyl unit/%	Carboxylated unit/%	Anchor unit/%
MGlu-HPG10	0	100	–
MGlu-HPG20	0	100	–
MGlu-HPG40	0	100	–
MGlu-HPG60	5	95	–
Linear MGluPG76	10	90	–
Linear MGluPG222	6	94	–
MGlu-HPG10-C_{10}	0	88	12
MGlu-HPG20-C_{10}	0	90	10
MGlu-HPG40-C_{10}	0	90	10
MGlu-HPG60-C_{10}	5	85	10
Linear MGluPG76-C_{10}	10	75	15
Linear MGluPG222-C_{10}	9	81	10

Please cite this article as: E. Yuba, et al., Carboxylated hyperbranched poly(glycidol)s for preparation of pH-sensitive liposomes, J. Control. Release (2010), doi:10.1016/j.jconrel.2010.03.001

carboxylated poly(glycidol) chain is sufficient to fix the polymer chain onto an EYPC liposome membrane [5,7]. Based on previous studies, 1-aminodecane was combined to about 10 unit% of the polymer chains in this study (Table 1).

Acid–base titration of these polymers was performed to estimate the p*K*a values. As presented in Table 2, MGlu-HPGs had p*K*a values around 5.9–6.5 and p*K*a slightly increased concomitantly with increasing DP. For polymers with a hyperbranched structure, their chain density increases concomitantly with increasing DP. Therefore, hydrophobic interactions among these crowded polymer chains of HPG with higher DP might engender a more compact conformation. Such a compact conformation of HPGs increases spatial density of carboxyl groups in the polymer chains, which might suppress dissociation of carboxyl groups to avoid repulsive electrostatic forces among carboxylate anions. In addition, hydrophobic environment of the crowded polymer chains may induce suppression of dissociation of carboxyl groups. As a result, p*K*a of the MGlu-HPGs might increase with increasing DP.

Hydrophobicity of carboxylated polymers affects their precipitation behaviors [20]. For that reason, we estimated the pH at which the polymers precipitate by measuring optical densities of these polymer solutions at varying pHs (Fig. 2). These polymers were soluble in water at neutral pH; their solutions were transparent. However, the polymer solutions suddenly became turbid at a specific pH, which was defined as the precipitation pH. The precipitation pH thresholds for MGlu-HPGs were estimated as presented in Table 2. The precipitation pH shifted to slightly higher pH values with increasing DP of MGlu-HPGs, indicating that hydrophobicity of MGlu-HPG increases concomitantly with increasing DP, consistent with previous observations for methacrylic acid copolymers with varying hydrophobicities and a previous report by the authors [7,20]. Acid–base titration for these polymers revealed that the degree of protonation for their carboxyl groups was around 0.94–0.99 at the precipitation pH: most carboxyl groups must be protonated to elicit precipitation of these polymers.

Hydrophobicity of the polymers was further investigated using a fluorescence probe pyrene. An emission intensity ratio of the first (373 nm) to the third (384 nm) peaks of pyrene, I_1/I_3, is known to be sensitive to the micro-environmental polarity surrounding the pyrene molecule [21]. Consequently, this ratio has been widely used to estimate the hydrophobic nature of polymers [22,23]. Fig. 3 depicts the I_1/I_3 ratio of pyrene fluorescence in the buffer dissolving various polymers as a function of pH. In buffers dissolving MGlu-HPG10 or MGlu-HPG20, the I_1/I_3 ratios of pyrene were around 1.75 at pH 5, suggesting that these polymers formed few domains with a hydrophobic nature, even after protonation of carboxyl groups of the polymer chain. On the other hand, a significant decrease in the I_1/I_3 ratio is seen in the presence of MGlu-HPG40 or MGlu-HPG60 under weakly acidic conditions. These results suggest that MGlu-HPGs with higher DP formed more hydrophobic domains probably because of their globular structure. The presence of linear MGluPGs also affected the I_1/I_3 ratio, which tends to decrease below pH 6.0. However, their I_1/I_3 values were generally higher than those of MGlu-HPGs with similar DP. Linear MGluPGs might be unable to form hydrophobic domains as much as MGlu-HPGs because of their linear backbone structure.

Table 2
p*K*a and precipitation pH of various hyperbranched and linear poly(glycidol) derivatives.

Polymer	p*K*a	Precipitation pH	Degree of protonation at precipitation pH
MGlu-HPG10	5.9	4.4	0.98
MGlu-HPG20	6.2	4.6	0.98
MGlu-HPG40	6.5	4.7	0.99
MGlu-HPG60	6.5	4.9	0.94
Linear MGluPG76	6.2	4.9	0.99

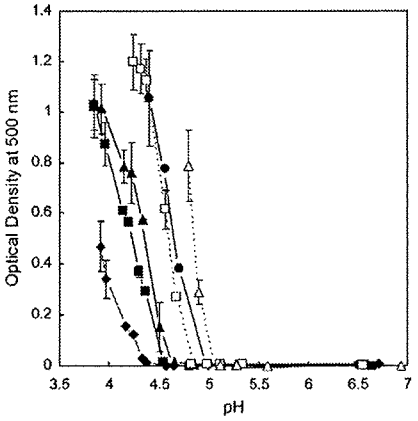

Fig. 2. Optical densities at 500 nm for solutions of MGlu-HPG10 (closed diamonds), MGlu-HPG20 (closed squares), MGlu-HPG40 (closed triangles), MGlu-HPG60 (closed circles), linear MGluPG76 (open triangles), and linear MGluPG222 (open squares) dissolved in 30 mM sodium acetate and 120 mM NaCl of various pHs (0.25 mg/mL) at 25 °C. Each point is the mean ± SD ($n = 3$).

3.2. Interaction of HPG derivatives with lipid membrane

We have shown that anchoring moiety into liposomes was necessary for poly(glycidol) derivatives to interact with liposomal membrane [7]. MGlu-HPG with anchor moieties (MGlu-HPG-C_{10}) were added to liposomes encapsulating both pyranine and its quencher DPX, and fluorescence of the released pyranine was monitored (Fig. 4). At neutral pH, no polymer showed a content release (Fig. 4A), indicating that these polymers did not disrupt liposome membrane under this condition. On the other hand, release of the contents was observed for all MGlu-HPG-C_{10} at pH 6.5 (Fig. 4B). Complete release was achieved below pH 6.0 (Fig. 4C), indicating that protonated polymers disrupt the liposome membrane. As portrayed in Fig. 4D, the content release in the weakly acidic region increased in the order of DP of MGlu-HPGs-C_{10}, indicating that the polymer with higher hydrophobicity triggers release more strongly. In addition, MGlu-HPGs-C_{10} triggered the content release more strongly

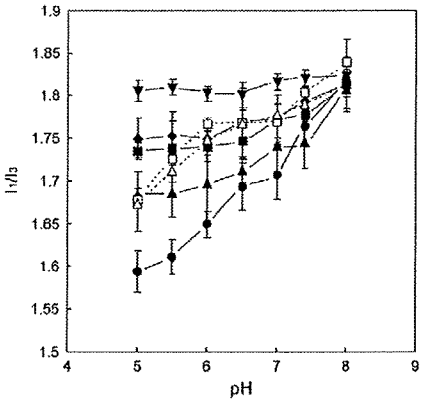

Fig. 3. pH-Dependence of I_1/I_3 of pyrene fluorescence in the absence (closed inverted triangles) or presence of MGlu-HPG10 (closed diamonds), MGlu-HPG20 (closed squares), MGlu-HPG40 (closed triangles), MGlu-HPG60 (closed circles), linear MGluPG76 (open triangles), and linear MGluPG222 (open squares) dissolving in 25 mM MES and 125 mM NaCl solution. Concentration of polymers and pyrene were 0.2 mg/mL and 1 μM, respectively. I_1/I_3 was defined as the fluorescence intensity ratio of the first band at 373 nm to the third band at 384 nm.

Please cite this article as: E. Yuba, et al., Carboxylated hyperbranched poly(glycidol)s for preparation of pH-sensitive liposomes, J. Control. Release (2010), doi:10.1016/j.jconrel.2010.03.001

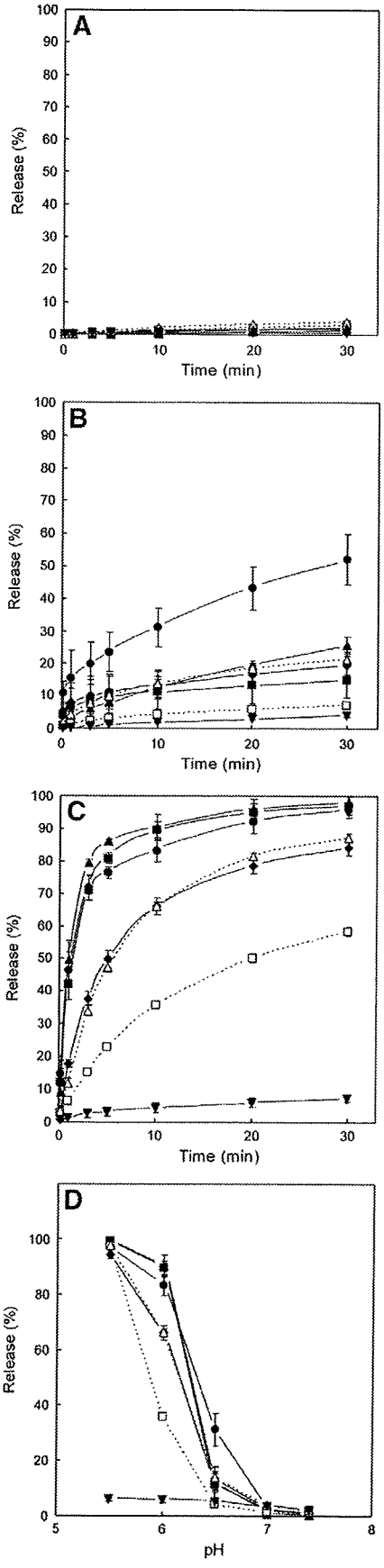

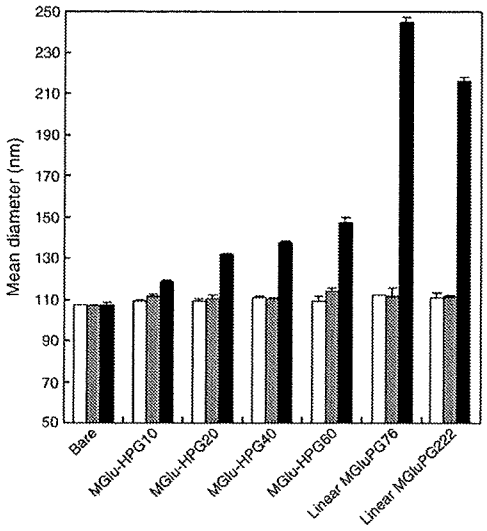

Fig. 5. Mean diameters of EYPC liposomes after overnight incubation with various polymers or without polymer at pH 7.4 (open bars), pH 6.5 (gray bars) and pH 5.5 (closed bars). Polymer and lipid concentrations were 0.11 mg/mL and 1.7×10^{-4} M, respectively. Each point is the mean ± SD ($n = 3$).

than linear MGluPG-C_{10} under the weakly acidic condition, demonstrating that the hyperbranched polymers can destabilize the liposome membrane more strongly than linear polymers.

Interaction of the polymers with the liposomes was also investigated through inspection of the liposome size change. EYPC liposomes were incubated with MGlu-HPGs-C_{10} or linear MGluPGs-C_{10} at various pHs overnight; their diameters were evaluated by DLS (Fig. 5). The liposome size changed only slightly after incubation with MGlu-HPGs-C_{10} at pHs 7.4 and 6.5, but incubation at pH 5.5 increased their diameter to some extent. This range of increase rose with increasing DP. On the other hand, incubation with linear MGluPGs-C_{10} induced remarkable liposome size change at pH 5.5. Because linear MGluPG-C_{10} has a high degree of freedom on their conformation, they might promote intervesicular interaction, engendering aggregation of liposomes. In contrast, MGlu-HPGs-C_{10} might interact with the membrane in a single liposome because of their compact conformation.

3.3. Preparation of pH-sensitive liposomes using HPG derivatives

Fig. 6 depicts pH-sensitive content release behaviors of liposomes modified with MGlu-HPGs-C_{10} or linear MGluPGs-C_{10}. All liposomes retained pyranine at pH 7.4 (Fig. 6A). However, MGlu-HPGs-C_{10}-modified liposomes enhanced their content release below pH 6.0; an almost complete release was achieved at pH 5.5 (Fig. 6B and C). As portrayed in Fig. 6D, liposomes modified with MGlu-HPGs-C_{10} of low DP exhibited higher content release in acidic pH than MGlu-HPGs-C_{10} of high DP. These observations differ from the case of content release induced by the addition of these polymers into the liposome suspensions (Fig. 4). These might be resulted from the difference of protonation behavior of polymers between the liposome surface and in an aqueous medium. It is possible that the protonation of MGlu-HPG-C_{10} with low DP is enhanced on the

Fig. 4. Pyranine release from EYPC liposomes induced by various hyperbranched poly (glycidol) derivatives. Time courses at pH 7.4 (A), pH 6.5 (B), and pH 6.0 (C), and pH-dependence (D) of pyranine release induced by MGlu-HPG10 (closed diamonds), MGlu-HPG20 (closed squares), MGlu-HPG40 (closed triangles), MGlu-HPG60 (closed circles), linear MGluPG76 (open triangles), and linear MGluPG222 (open squares) or without polymer (closed and inverted triangles). Percent release of pyranine after 10 min-incubation was shown (D). Polymer and lipid concentrations were 0.013 mg/mL and 2.0×10^{-5} M, respectively. Each point is the mean ± SD ($n = 3$).

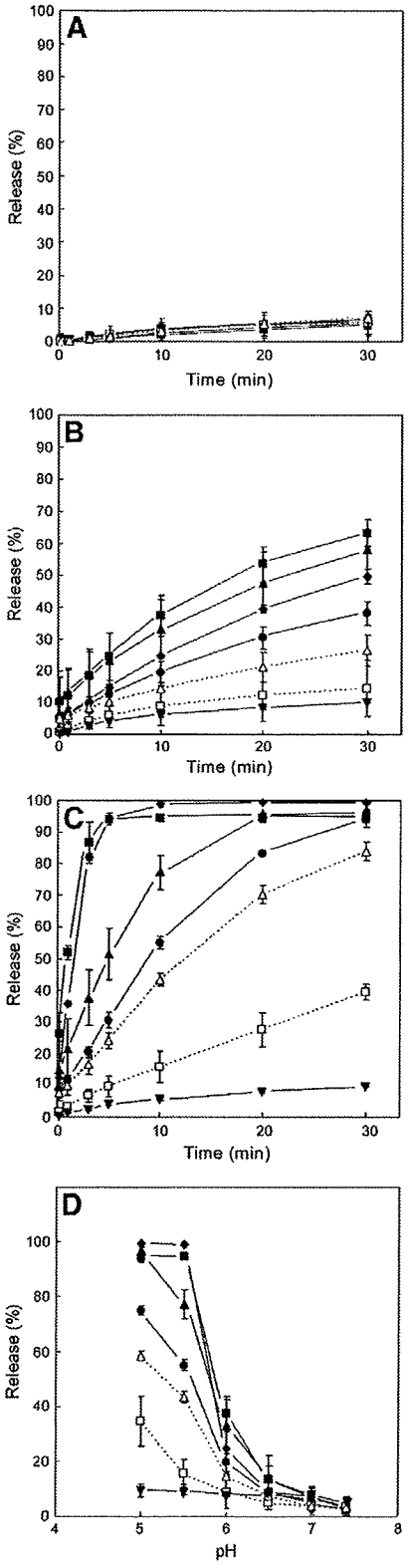

Fig. 6. Pyranine release from EYPC liposomes modified with various hyperbranched and linear poly(glycidol) derivatives. Time courses at pH 7.4 (A), pH 6.0 (B), and pH 5.5 (C), and pH-dependence (D) of pyranine release from EYPC liposomes modified with MGlu-HPG10 (closed diamonds), MGlu-HPG20 (closed squares), MGlu-HPG40 (closed triangles), MGlu-HPG60 (closed circles), linear MGluPG76 (open triangles), linear MGluPG222 (open squares), and unmodified EYPC liposomes (closed and inverted triangles). Percent release of pyranine after 10 min-incubation was shown (D). Lipid concentrations were 2.0×10^{-5} M. Each point is the mean ± SD ($n=3$).

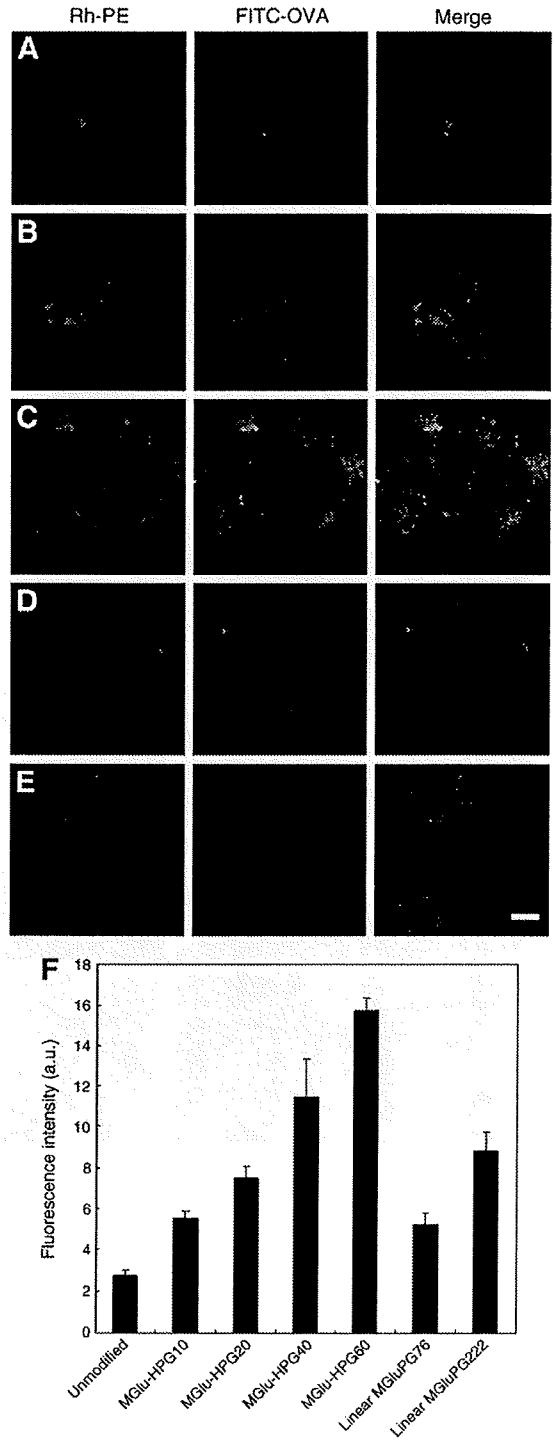

Fig. 7. Confocal laser scanning microscopic (CLSM) images of DC2.4 cells treated with Rh-PE-labeled and FITC-OVA-loaded EYPC liposomes of various types: plain liposomes (A); liposomes modified with MGlu-HPG20-C_{10} (B), MGlu-HPG60-C_{10} (C), linear MGluPG76-C_{10} (D), or linear MGluPG222-C_{10} (E). FITC-OVA concentration was 50 μg/mL. Intracellular localization of Rh-PE (red) and FITC-OVA (green) was observed using a CLSM. Scale bar represents 10 μm. (F) Fluorescence intensities of DC2.4 cells treated with Rh-PE-labeled EYPC liposomes modified with or without polymers of various types. The fluorescence intensities of Rh-PE were determined by flow cytometry. (For interpretation of the references to color in this figure legend, the reader is referred to the web version of this article.)

Please cite this article as: E. Yuba, et al., Carboxylated hyperbranched poly(glycidol)s for preparation of pH-sensitive liposomes, J. Control. Release (2010), doi:10.1016/j.jconrel.2010.03.001

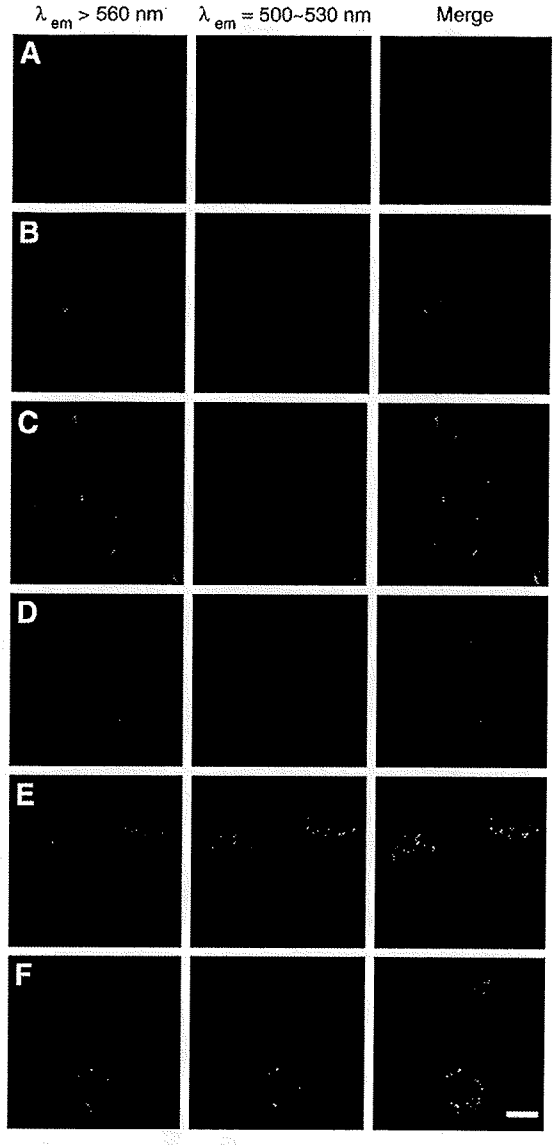

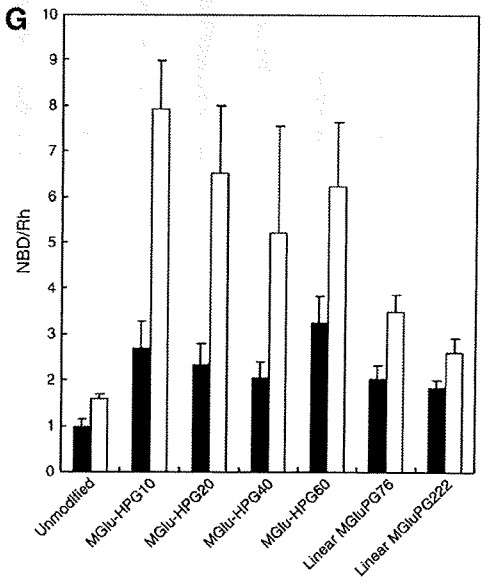

liposome membrane because carboxylate anions of the small-size polymer might exist in close vicinity of the membrane. Comparison of liposomes modified with linear and hyperbranched polymers shows that MGlu-HPG-C_{10}-modified liposomes induced the content release in a higher pH region than linear MGluPG-C_{10}-modified liposomes. Therefore, the liposomes having the hyperbranched polymers might destabilize the endosome in the early stage of endocytic pathway after their uptake by a cell.

3.4. Cytoplasmic delivery by polymer-modified liposomes

Previously, we have shown that liposomes modified with linear MGluPG can be used for cytoplasmic delivery of antigenic proteins, such as OVA, into dendritic cells for the induction of antigen-specific immune responses [24]. Therefore, we compared the performance of the MGlu-HPG-modified liposomes as antigenic protein delivery vehicles with that of the linear MGluPG-modified liposomes.

We prepared the MGlu-HPGs-C_{10}-modified liposomes labeled with Rh-PE and loaded with FITC–OVA, and their interaction with DC2.4 cells was compared with that for the linear MGluPG-C_{10}-modified EYPC liposomes or bare EYPC liposomes labeled with Rh-PE and loaded with FITC–OVA. As presented in Fig. 7A, cells treated with the bare liposome displayed weak and punctate fluorescence of Rh-PE and FITC–OVA. Considering that the liposomes were generally taken up by a cell *via* endocytosis, it is highly likely that FITC–OVA molecules were still trapped in the endosome and/or lysosome. In contrast, cells treated with MGlu-HPG-C_{10}-modified liposomes showed punctate fluorescence of Rh-PE but diffuse fluorescence of FITC–OVA (Fig. 7B and C), indicating that lipid molecules existed in the endosome and lysosome but that FITC–OVA molecules existed in the cytoplasm. These liposomes have the capability of destabilizing lipid membranes under a weakly acidic environment. Therefore, it is likely that FITC–OVA molecules were transferred from the endosome into the cytoplasm. Furthermore, the fluorescence from cells treated with MGlu-HPG60-C_{10}-modified liposomes was much brighter than that from cells treated with MGlu-HPG20-C_{10}. Although diffuse fluorescence of FITC–OVA was also observed for cells treated with the linear MGluPG-C_{10}-modified liposomes (Fig. 7D and E), their fluorescence was weaker than the case of MGlu-HPG60-C_{10}-modified liposomes.

The Rh-fluorescence intensity of the liposome-treated cells was evaluated by flow cytometry (Fig. 7F). The Rh-fluorescence intensity increased concomitantly with increasing DP of MGlu-HPGs-C_{10}, indicating that liposomes modified with MGlu-HPG-C_{10} of higher DP were taken up more efficiently. In addition, cells treated with the MGlu-HPG60-C_{10}-modified liposomes showed higher intensity than those treated with the linear MGluPGs-C_{10}-modified liposomes. This result suggests that liposomes having polymers of a hyperbranched structure were taken up by cells more efficiently than those with the polymers of a linear structure. We have shown that linear MGluPG-modified liposomes are taken up by DC2.4 cells through their interaction with the cellular scavenger receptors, which recognize carboxylate anions of polymers [18,24]. Negatively charged carboxylate groups of the hyperbranched polymer tend to locate in the peripheral region of the polymer. Therefore, these groups might be recognized by scavenger receptors efficiently, thereby promoting their uptake by the cells. These results demonstrate that modification

Fig. 8. CLSM images of DC2.4 cells treated with EYPC (A–C) or EYPC/DOPE (1/1, mol/mol) (D–F) plain liposomes (A, D) or liposomes modified with MGlu-HPG60-C_{10} (B, E), and linear MGluPG76-C_{10} (C, F). Liposomal lipid concentration was 0.5 mM. Fluorescence of NBD-PE and Rh-PE upon excitation at 488 nm was observed using a CLSM. Scale bar represents 10 μm. (G) Fluorescence intensity ratios of NBD-PE to Rh-PE for DC2.4 cells treated with EYPC (closed symbols) or EYPC/DOPE (open symbols) liposomes modified with or without polymers. Fluorescence intensity ratios were evaluated by flow cytometry and were expressed as relative values using the ratio of the plain EYPC liposome-treated cells as the standard.

Please cite this article as: E. Yuba, et al., Carboxylated hyperbranched poly(glycidol)s for preparation of pH-sensitive liposomes, J. Control. Release (2010), doi:10.1016/j.jconrel.2010.03.001

of liposomes with MGlu-HPG-C_{10} can produce pH-sensitive liposomes that achieve efficient cytoplasmic delivery of proteins.

3.5. Fusion of polymer-modified liposomes within cell

Finally, we attempted to verify the fusion of MGlu-HPG-C_{10}-modified liposomes in the cells. The polymer-modified liposomes containing NBD-PE and Rh-PE were prepared to detect the fusion of the liposomes with intracellular membranes [6,25]. Fusion of the labeled liposomes with endosomal membranes causes dilution of these fluorescent lipids in the membrane, resulting in a decrease of energy transfer efficiency between these fluorescent lipids.

The fluorescent lipid-labeled liposomes with or without polymers were applied to DC2.4 cells and incubated for 4 h. Then cellular fluorescence was observed using a CLSM under irradiation of light with a wavelength of 488 nm, which is for excitation of NBD-PE (Fig. 8). As Fig. 8A shows, cells treated with the bare liposomes displayed only the fluorescence of Rh-PE, suggesting that the fluorescence of NBD-PE was quenched by energy transfer to Rh-PE and hence the bare liposomes did not fuse with the endosomal membrane. In contrast, the cells treated with MGlu-HPG60-C_{10}-modified or linear MGluPG76-C_{10}-modified liposomes exhibited not only Rh-PE-fluorescence but also NBD-PE-fluorescence, indicating that the fusion between these liposomes and the endosomal membranes occurred (Fig. 8B and C). However, the fluorescence of NBD-PE was very weak, suggesting that their fusion was not efficient.

The intracellular fusion behavior of the liposomes containing a non-bilayer-forming lipid DOPE, which is known to enhance membrane fusion, was also examined (Figs. 8D–F). For cells treated with the bare EYPC/DOPE liposomes, fluorescence of NBD-PE remained very weak (Fig. 8D). However, intensive fluorescence of NBD-PE was detected from cells treated with the DOPE-containing liposomes having either MGlu-HPG60-C_{10} or linear MGluPG76-C_{10}, indicating that these polymer-modified liposomes fused efficiently with endosomal membranes (Figs. 8E and F).

The fluorescence intensity ratios of NBD-PE to Rh-PE for the liposome-treated cells were evaluated by flow cytometry and were expressed as relative values using the ratio of the bare EYPC liposome-treated cells as the standard (Fig. 8G). The cells treated with either polymer-modified EYPC liposomes showed a 2–3 times increase in the NBD/Rh ratio compared with those treated with the base EYPC liposomes. Furthermore, no significant difference was found between the cells treated with any MGlu-HPG-C_{10}-modified and linear MGluPG-C_{10}-modified EYPC liposomes. These results indicate that these polymer-modified EYPC liposomes possess similar abilities to fuse with the endosomal membrane. Indeed, the EYPC/DOPE liposomes modified with these polymers caused a more significant increase in the NBD/Rh ratio than EYPC liposomes having the same polymers (Fig. 8G). In particular, the EYPC/DOPE liposomes modified with the hyperbranched polymers showed a higher NBD/Rh ratio than linear polymers, indicating that the backbone structure of the polymer affects their ability to generate the fusion ability of EYPC/DOPE liposomes.

The performance of MGlu-HPG-modified liposomes as a cytoplasmic delivery system was shown to increase as MGlu-HPG with higher DP was used for liposome modification. There might be various modes of interaction between MGlu-HPG with lipid membranes, such as absorption onto the membrane, penetration into the membrane, and solubilization lipid molecules. Therefore, their ability to destabilize lipid membranes might be influenced by their size. Optimization of molecular size may generate MGlu-HPG-modified liposomes with even higher performance.

4. Conclusion

A new type of pH-sensitive polymer with a hyperbranched backbone—MGlu-HPG-C_{10}—was synthesized. Its feasibility for the production of pH-sensitive liposomes was then investigated. Their ability for pH-sensitization of liposomes was enhanced with increasing DP. Modification of liposomes with MGlu-HPG-C_{10} produced highly pH-sensitive liposomes that undergo content release at mildly acidic pH. The MGlu-HPG-C_{10}-modified liposomes encapsulating OVA delivered their contents efficiently into the cytosol of DC2.4 cells. Especially, liposomes having MGlu-HPG-C_{10} with high DP exhibited higher fusion ability and more efficient cellular internalization property than the liposomes modified with the counterpart polymers with a linear backbone structure. This is the first report describing the importance of the polymer backbone structure for polymer-based functionalization of liposomes. The MGlu-HPG-C_{10}-modified liposomes showed an excellent ability to deliver the loaded proteins into the cytosol of dendritic cell-derived cells. Therefore, they might have potential usefulness for the delivery of antigenic proteins.

Acknowledgments

This work was supported in part by a Grant-in-Aid for Research on Nanotechnical Medicine from the Ministry of Health, Labor and Welfare of Japan and by a Grant-in-aid for Scientific Research from the Ministry of Education, Science, Sports, and Culture in Japan. E. Yuba thanks the Research Fellowships of the Japan Society for the Promotion of Science for Young Scientists.

References

[1] D. Liu, L. Huang, pH-Sensitive, plasma-stable liposomes with relatively prolonged residence in circulation, Biochim. Biophys. Acta 1022 (1990) 348–354.
[2] H. Ellens, J. Bentz, F.C. Szoka, pH-Induced destabilization of phosphatidylethanolamine-containing liposomes: role of bilayer contact, Biochemistry 23 (1984) 1532–1538.
[3] J. Kunisawa, T. Nakanishi, I. Takahashi, A. Okudaira, Y. Tsutsumi, K. Katayama, S. Nakagawa, H. Kiyono, T. Mayumi, Sendai virus fusion protein mediates simultaneous induction of MHC class I/II-dependent mucosal and systemic immune responses via the nasopharyngeal-associated lymphoreticular tissue immune system, J. Immunol. 167 (2001) 1406–1412.
[4] K. Seki, D.A. Tirrell, pH-Dependent complexation of poly(acrylic acid) derivatives with phospholipid vesicle membrane, Macromolecules 17 (1984) 1692–1698.
[5] K. Kono, K. Zenitani, T. Takagishi, Novel pH-sensitive liposomes: liposomes bearing a poly(ethylene glycol) derivative with carboxyl groups, Biochim. Biophys. Acta 1193 (1994) 1–9.
[6] K. Kono, T. Igawa, T. Takagishi, Cytoplasmic delivery of calcein mediated by liposomes modified with a pH-sensitive poly(ethylene glycol) derivative, Biochim. Biophys. Acta 1325 (1997) 143–154.
[7] N. Sakaguchi, C. Kojima, A. Harada, K. Kono, Preparation of pH-sensitive poly (glycidol) derivatives with varying hydrophobicities: their ability to sensitize stable liposomes to pH, Bioconjugate Chem. 19 (2008) 1040–1048.
[8] P.A. Bullough, F.M. Hughson, J.J. Skehel, D.C. Wiley, Structure of influenza haemagglutinin at the pH of membrane fusion, Nature 371 (1994) 37–43.
[9] N. Murthy, J.R. Robichaud, D.A. Tirrell, P.S. Stayton, A.S. Hoffman, The design and synthesis of polymers for eukaryotic membrane disruption, J. Controlled Release 61 (1999) 137–143.
[10] C.A. Lackey, N. Murthy, O.W. Press, D.A. Tirrell, A.S. Hoffman, P.S. Stayton, Hemolytic activity of pH-responsive polymer-streptavidin bioconjugates, Bioconjugate Chem. 10 (1999) 401–405.
[11] C.C. Lee, J.A. MacKay, J.M.J. Frechet, F.C. Szoka, Designing dendrimers for biological applications, Nat. Biotechnol. 12 (2005) 1517–1526.
[12] U. Boas, P.M.H. Heegaad, Dendrimers in drug research, Chem. Soc. Rev. 33 (2004) 43–63.
[13] A. Sunder, R. Mulhaupt, R. Haag, H. Frey, Hyperbranched polyether polyols: a modular approach to complex polymer architectures, Adv. Mater. 12 (2000) 235–239.
[14] A. Sunder, J. Heinemann, H. Frey, Controlling the growth of polymer trees: concepts and perspectives for hyperbranched polymers, Chem. Eur. J. 6 (2000) 2499–2506.
[15] H. Frey, R. Haag, Dendritic polyglycerol: a new versatile biocompatible material, Rev. Mol. Biotechnol. 90 (2002) 257–267.
[16] Z. Shen, G. Reznikoff, G. Dranoff, K.L. Rock, Cloned dendritic cells can present exogenous antigens on both MHC class I and class II molecules, J. Immunol. 158 (1997) 2723–2730.
[17] D.L. Daleke, K. Hong, D. Papahadjopoulos, Endocytosis of liposomes by macrophages: binding, acidification and leakage of liposomes monitored by a new fluorescence assay, Biochim. Biophys. Acta 1024 (1990) 352–366.
[18] E. Yuba, C. Kojima, N. Sakaguchi, A. Harada, K. Koiwai, K. Kono, Gene delivery to dendritic cells mediated by complexes of lipoplexes and pH-sensitive fusogenic polymer-modified liposomes, J. Controlled Release 130 (2008) 77–83.
[19] R.D. Hester, P.H. Mitchell, A new universal GPC calibration method, J. Polym. Sci. Chem. Ed. 18 (1980) 1727–1738.

[20] M.A. Yassine, M. Lafleur, C. Meier, H.U. Petereit, J.C. Leroux, Characterization of the membrane-destabilizing properties of different pH-sensitive methacylic acid copolymers, Biochim. Biophys. Acta 1613 (2003) 28–38.
[21] K. Kalyanasundaram, J.K. Thomas, Environmental effects on vibronic band intensities in pyrene monomer fluorescence and their application in studies of micellar systems, J. Am. Chem. Soc. 99 (1977) 2039–2044.
[22] H.G. Schild, D.A. Tirrell, Microheterogeneous solutions of amphiphilic copolymers of N-isopropylacrylamide. An investigation via fluorescence methods, Langmuir 7 (1991) 1319–1324.
[23] K. Tamano, T. Imae, S. Yusa, Y. Shimada, Structure-selective dye uptake into an aggregate of a copolymer with linear polyelectrolyte block and hydrophobic block carrying pendant dendritic moiety in water, J. Phys. Chem. B 109 (2005) 1226–1230.
[24] E. Yuba, C. Kojima, A. Harada, Tana, S. Watarai, K. Kono, pH-Sensitive fusogenic polymer-modified liposomes as a carrier of antigenic proteins for activation of cellular immunity, Biomaterials 31 (2010) 943–951.
[25] D.K. Struck, D. Hoekstra, R.E. Pagano, Use of resonance energy transfer to monitor membrane fusion, Biochemistry 20 (1981) 4093–4099.

Please cite this article as: E. Yuba, et al., Carboxylated hyperbranched poly(glycidol)s for preparation of pH-sensitive liposomes, J. Control. Release (2010), doi:10.1016/j.jconrel.2010.03.001

ARTICLES

Multimodal Silica-Shelled Quantum Dots: Direct Intracellular Delivery, Photosensitization, Toxic, and Microcirculation Effects

Rumiana Bakalova,*,† Zhivko Zhelev,† Ichio Aoki,† Kazuto Masamoto,† Milka Mileva,‡ Takayuki Obata,† Makoto Higuchi,† Veselina Gadjeva,§ and Iwao Kanno†

Molecular Imaging Center, National Institute of Radiological Sciences (NIRS), 4-9-1 Anagawa, Chiba 263-8555, Japan, Department of Medical Physics and Biophysics, Medical University, Sofia, Bulgaria, and Department of Chemistry and Biochemistry, Medical Faculty, Thracian University, Stara Zagora, Bulgaria. Received November 28, 2007; Revised Manuscript Received March 13, 2008

In the present study, we describe a multimodal QD probe with combined fluorescent and paramagnetic properties, based on silica-shelled single QD micelles with incorporated paramagnetic substances [tris(2,2,6,6-tetramethyl-3,5-heptanedionate)/gadolinium] into the micelle and/or silica coat. The probe was characterized with high photoluminescence quantum yield and good positive MRI contrast, low cytotoxicity, and easy intracellular delivery in viable cells. The intravenous administration of the probe in experimental animals did not affect significantly the physiological parameters and microcirculation (e.g., heart rate, blood pressure, diameter and shape of blood vessels), which makes it appropriate for tracing of blood circulation and *in vivo* multimodal imaging using fluorescent confocal microscopy, two-photon microscopy, and MRI.

INTRODUCTION

The careful design of the architecture of water-soluble QDs enables the creation of nanobioprobes that are compatible with several imaging techniques, so-called multimodal imaging. This opens the door to the existing prospect of simultaneous imaging of QD probes by a variety of techniques including optical imaging, magnetic resonance imaging (MRI), positron emission tomography (PET), computed tomography (CT), and X-ray imaging.

In particular, by fabricating QD probes that exhibit both fluorescent and paramagnetic properties, optical imaging and MRI can be used in a complementary fashion. This is a powerful combination, as the MRI offers an ability to follow the distribution of molecules *in vivo* or provide an anatomical reference, whereas the optical imaging can be applied to obtain detailed information at subcellular levels. The potential applications include monitoring tissue implants and studying the real-time dynamics of tumor metastases and biochemical mediators that might be responsible for many diseases.

The use of a single multimodal probe with two or more imaging techniques has several advantages. The conventional (nonmultimodal) probes, used in PET, MRI, or optical imaging, have different structures and properties, which determine their different target affinity and pharmacodynamics in the organism. Often, the target can be detected by several imaging techniques using several imaging probes with different properties and pharmacodynamics, so the results cannot be easily compared and verified. The researchers and clinicians are faced with the dilemma of which technique to choose and which data to accept as true. The use of a single multimodal probe with two or more imaging techniques minimizes the artifacts and enables a precise comparative analysis of the images, obtained by different techniques.

The existing prospect of using QDs as multimodal imaging probes attracts the interest of researchers in many different scientific fields, and the number of publications on the topic has increased exponentially in recent years (*1*–*21*). However, so far, the results are preliminary and interpretations are still speculative, especially in terms of *in vivo* deep-tissue imaging.

Perhaps the most attractive for development of multimodal imaging probes (optical and paramagnetic) are silica-shelled QDs. The silica is a bioinert material. The silica shell enables incorporation of a large amount of contrast substances inside the silica sphere (e.g., CdSe, CdTe, CdS, InAs, or InP QDs and Fe_2O_3, Fe_3O_4, $CoFe_2O_4$, $MnFe_2O_4$, FePt, or $CoPt_3$ paramagnetic nanoparticles; fluorescent/paramagnetic heterodimers, such as Fe_3O_4-Au, CoPt-Au, FePt-Ag, Fe_3O_4-Au-PbSe, γ-Fe_2O_3-CdS, FePt-CdS, Co/CdS core/shell, Co/CdSe core/shell, CdSe/Zn_{1-x}-Mn_xS; QDs and paramagnetic fatty acids) (*3, 7, 13, 15, 16*). In addition, paramagnetic substances (e.g., chelators for gadolinium, manganese, etc.) could also be attached on the surface of silica-coated QDs (*5, 15, 18*–*20*). The high fluorescent contrast (as a result of high quantum yield of QDs) and the high paramagnetic contrast (as a result of incorporation of a large amount of paramagnetic substances in the small volume of the silica sphere) enable development of a probe that could be detected *in vivo* in a single manner, simultaneously using optical imaging and MRI. In that case, even single cells and molecular targets could be visualized.

* Rumiana Bakalova, PhD, Department of Biophysics, Molecular Imaging Center, National Institute of Radiological Sciences (NIRS), 4-9-1 Anagawa, Chiba 263-8555, Japan. Tel.: +81-43-206-4067. Fax: +81-43-206-3276 . E-mail: bakalova@nirs.go.jp.

† NIRS.

‡ Medical University, Sofia, Bulgaria.

§ Thracian University.

10.1021/bc700431c CCC: $40.75
Published on Web 05/22/2008

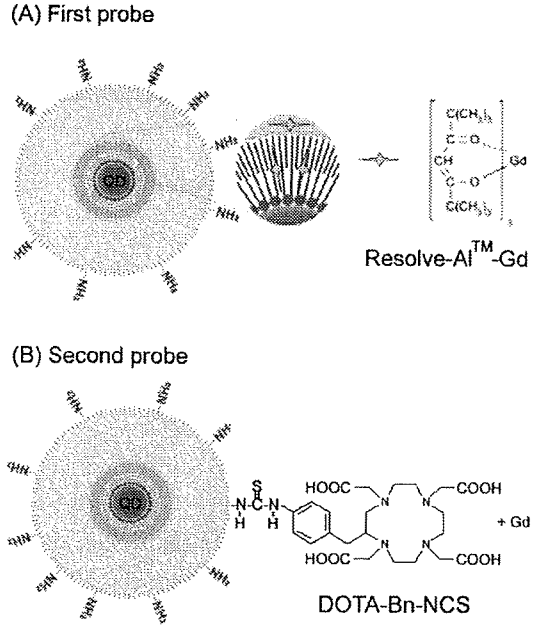

Figure 1. Structure of multimodal silica-shelled QD probes. In the first probe (A), the gadolinium complex is incorporated into the silica coat and/or hydrophobic micelle around the QD. In the second probe (B), the gadolinium complex is conjugated on the surface of silica sphere.

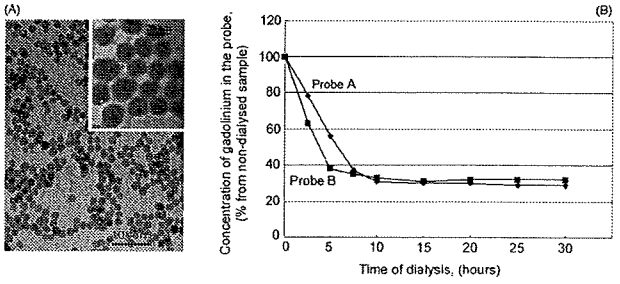

(C) Spectral characteristics of probes (A) and (B).

Spectral characteristic	Probe (A)	Probe (B)
PL QY (%)		
- in distilled water	~35-50	~35-50
- in 10 mM PBS, pH 7.4	~30-45	~32-48
- in 20 mM Tris-HCl, pH 7.4	~27-45	~25-45
T_1 (ms)	264.2 +/- 5.6	281.0 +/- 19.2
T_2 (ms)	80.0 +/- 0.8	142.5 +/- 2.8

Figure 2. (A) Transmission electron micrographs of silica-shelled QD micelles. (B) Retention of gadolinium complex in the silica sphere (probe A) or on the surface of the silica sphere (probe B) after purification via dialysis. (C) Fluorescent and paramagnetic characteristics of probes A and B. The probes were purified using 48 h dialysis. Longitudinal relaxation time (T_1) and transverse relaxation time (T_2) were calculated at equal concentrations of both probes (corresponding to 500 nM QDs). The QD concentration was calculated from the absorbance spectra of multimodal silica-shelled QDs, using the equation of Yu et al. (*38*). The MRI measurements were performed in a 4.7 T magnet (General Electric, CT) interfaced to a Bruker Avance console (Bruker Medical GmbH, Germany). A 30 mm diameter Litz coil (Doty Scientific Inc., SC, USA) was used for measurement of the samples. The sample temperature was maintained at room temperature (~22−24 °C). The measurements were performed in the following order: T_1-weighted imaging using conventional spin−echo (SE) sequence; multiecho SE imaging for T_2 calculations; and inversion−recovery SE imaging for T_1 calculations. For calculation of photoluminescence quantum yield (PL QY), the spectrally integrated emission of particle dispersion in different aqueous solutions (distilled water, PBS, or Tris buffer) was compared with the emission of an ethanol solution of rhodamine 6G (Fluka) of identical optical density (<0.015) at the excitation wavelength 365 nm.

The present study accents the biocompatibility of multimodal QD probes based on silica-shelled single QD micelles with incorporated gadolinium complexes into the micelle and/or silica coat. We tried to clarify the applicability of this probe for blood vessel tracing in the brain, estimating its effect on the major physiological characteristics (such as blood pressure, heart rate, and brain microcirculation) after *in vivo* intravenous (i.v.) administration.

EXPERIMENTAL PROCEDURES

Synthesis and Characterization of Multimodal QDs. Two multimodal QD-based probes were synthesized (Figure 1). The synthesis of the first probe (Figure 1A) was performed as it was described in our previous manuscripts (*21*). The synthesis of the second probe (Figure 1B) was performed according to refs 22, 23 (with slight modifications) (*22, 23*) Briefly, the gadolinium complex *S*-2-(4-isothiocyanatobenzyl)-1,4,7,10-tetraazacyclododecane tetraacetic acid/gadolinium (DOTA-Bn-NCS/gadolinium) was mixed with amino-functionalized QDs (400:1, mol/mol) in 10 mM PBS (pH 8.0). After 1 h incubation at room temperature, the conjugate was purified using dialysis, as described in our previous manuscript (*21*). DOTA-Bn-NCS/gadolinium complex was purchased from Macrocyclics Co. (USA). The same molar ratio gadolinium complex/QD = 400:1 was used in the synthesis of the first probe. After purification, the gadolinium concentration in the respective probe was measured using ^{1}H-MRI as described below. The structure and size of nanoparticles were characterized by TEM and DLS. Their spectral characteristics were measured using fluorescent spectroscopy, absorbance spectroscopy, and MRI.

Cell Cultures. HeLa cells were cultured in Minimum Essential Medium (MEM, GIBCO, Invitrogen, USA), supplemented with 10% inactivated FBS (Sanko, Japan). A-549 cells, derived from human lung cancer, Jurkat and K-562 cell lines, derived from human acute lymphoblastic leukemia or chronic myeloid leukemia, respectively, were cultured in RPMI-1640 medium (GIBCO, Invitrogen, USA), supplemented with 10% inactivated FBS (Sanko, Japan), 100 U/mL penicillin (GIBCO, Invitrogen, USA), and 100 μg/mL streptomycin (GIBCO, Invitrogen, USA). One day before the treatment with QDs, the cells (1×10^5 cells/mL) were dispensed in 100 μL aliquots in 96-well plates and cultured overnight in medium without FBS and antibiotics, in humidified atmosphere (5% CO_2, 37 °C).

Intracellular Delivery of Multimodal QDs (MRI Measurements and Data Analysis). The MRI measurements were performed in a 4.7 T magnet (General Electric, CT) or a 7.0 T magnet (Kobelco, Japan) interfaced to a Bruker Avance console (Bruker Medical GmbH, Germany). A 30 mm diameter Litz coil (Doty Scientific Inc., SC, USA) or 70 mm diameter volume coil (Bruker) was used for measurement of the samples. The details are indicated in the figure captions. The PCR tubes were mounted on a plastic holder for 4.7 T or on a 70 mm diameter volume coil for 7.0 T and set in the center of the coil. The sample temperature was maintained at room temperature (approximately 22−24 °C). The measurements were performed in the following order: T_1 weighted imaging, using conventional spin−echo (SE) sequence; multiecho SE imaging for T_2 calculations; and inversion−recovery SE imaging for T_1 calculations.